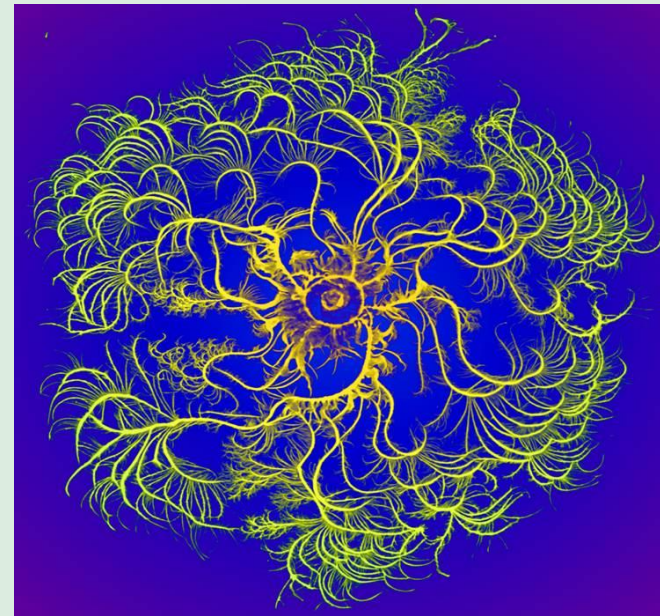


Chaos, Fractals, Multifractals: The Complexity of Life



KSMB-SMB Satellite Workshop, 27 June 2024
Mogens H. Jensen, Niels Bohr Institute



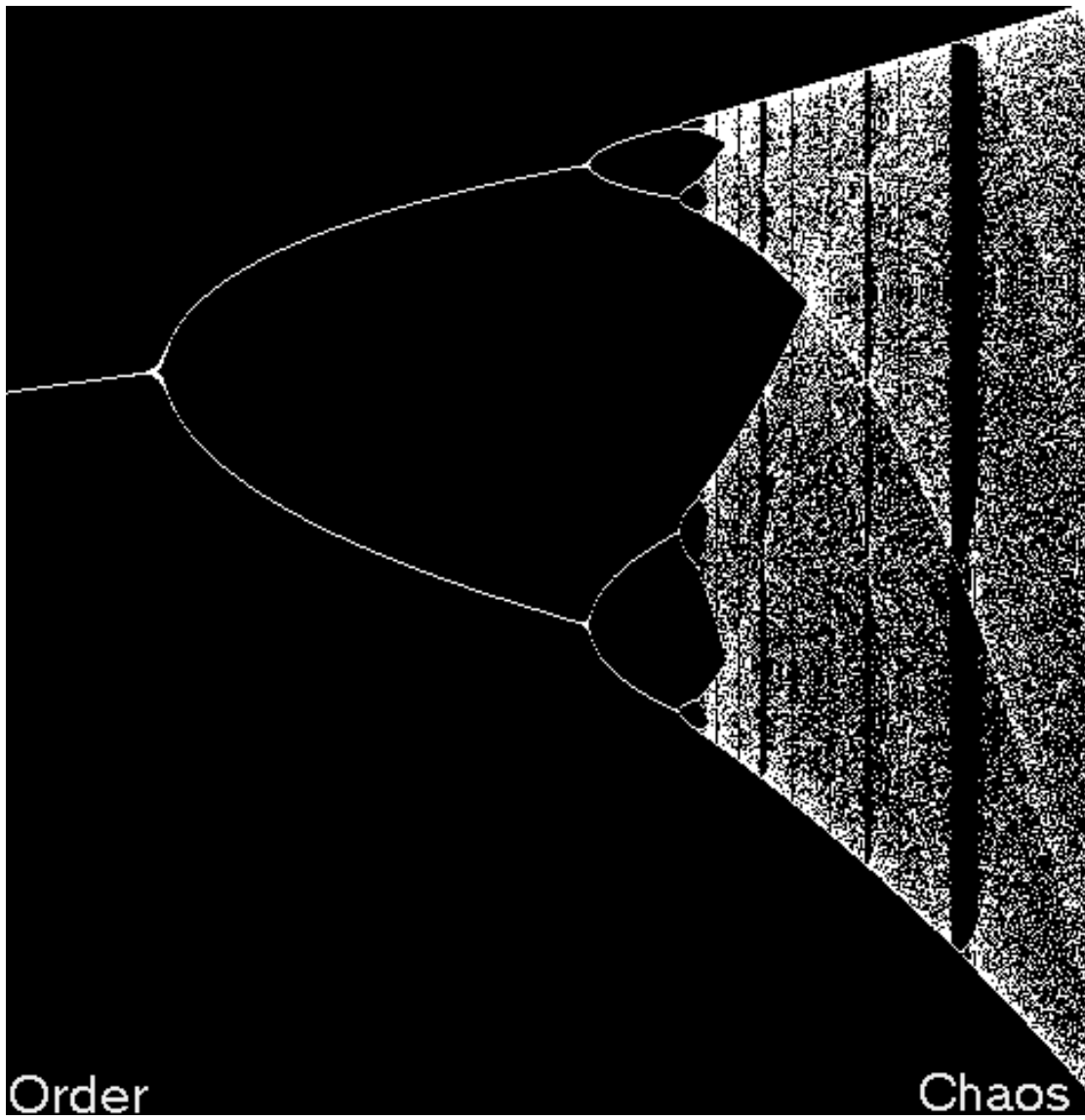
- Chaos
- Fractals
- Multifractals
- Universality from experiments
- Fractal aggregates
- Avalanches
- Biological networks
- Proteins, Genetics
- Social science, paradigms



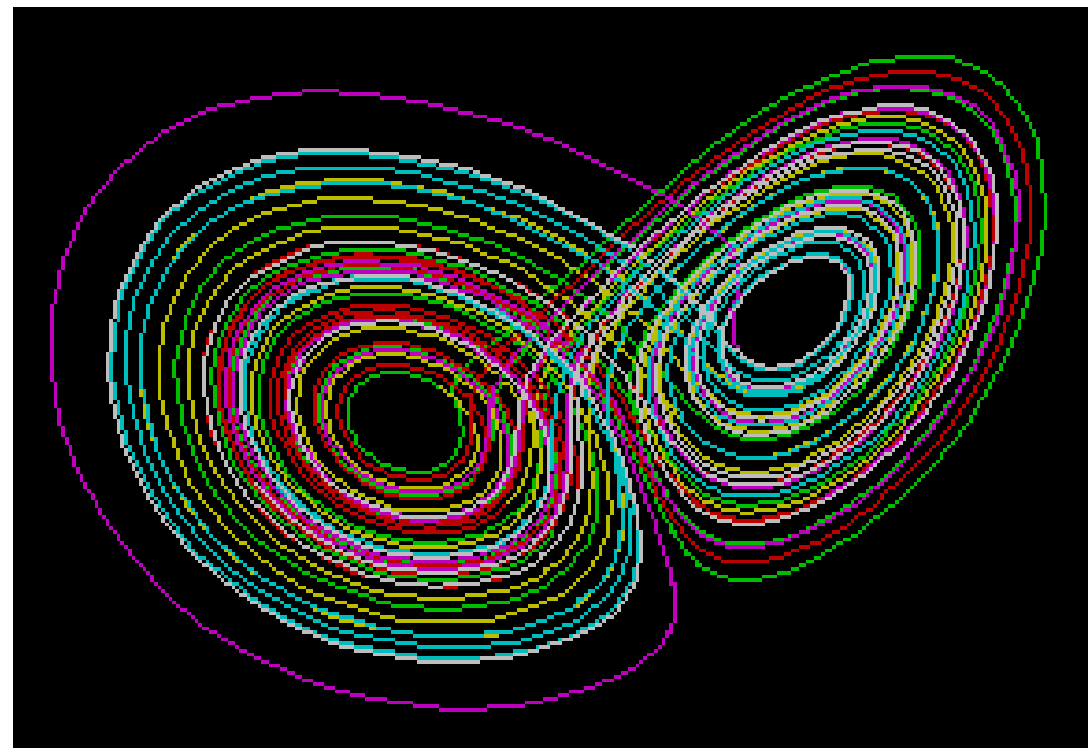
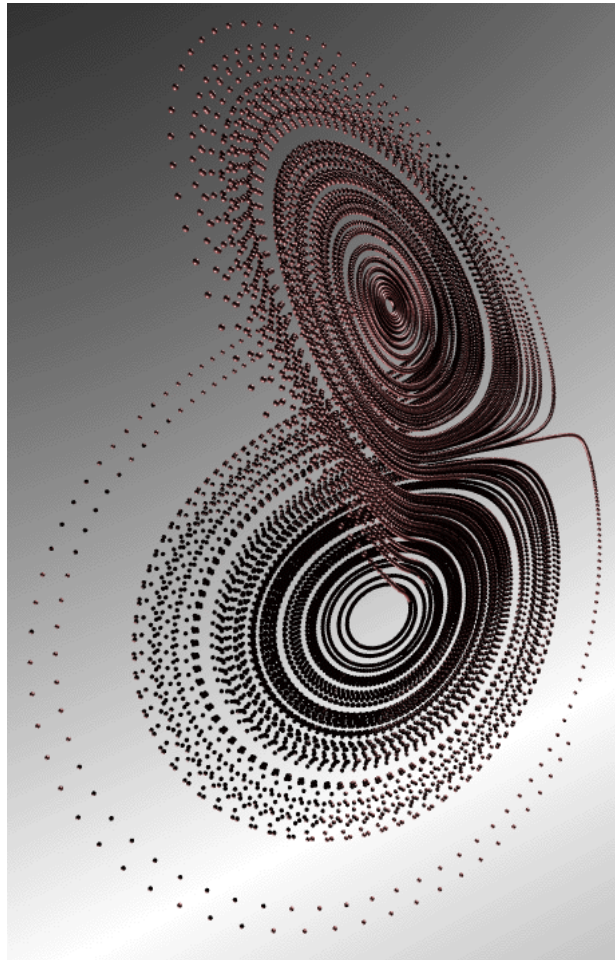
Complex dynamics – chaos !



Bifurcation tree !

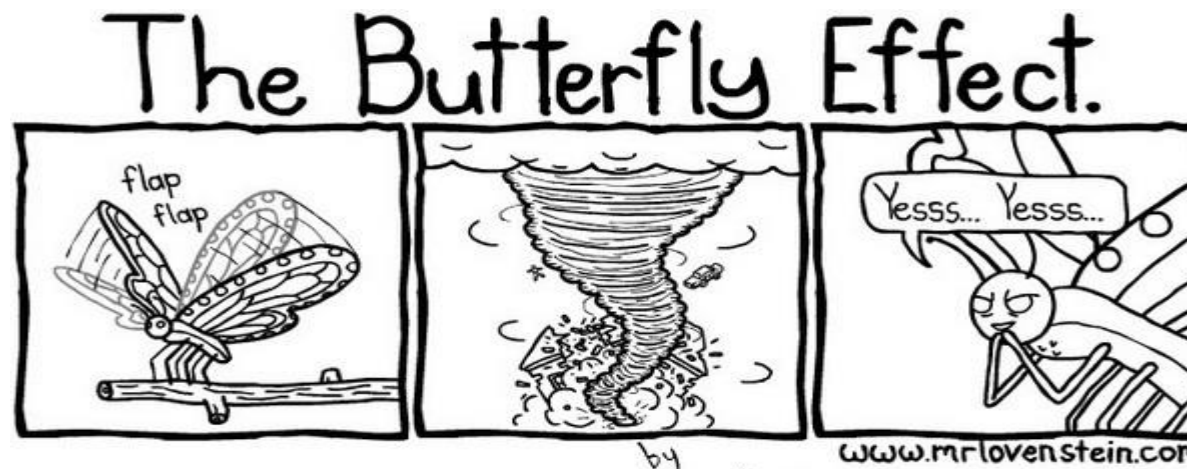


Strange attractors: Non-periodic motion: Sensitive Dependence on initial conditions !



The 'butterfly effect':

A butterfly moving its wing over Brazil
may cause a tornado over Florida !

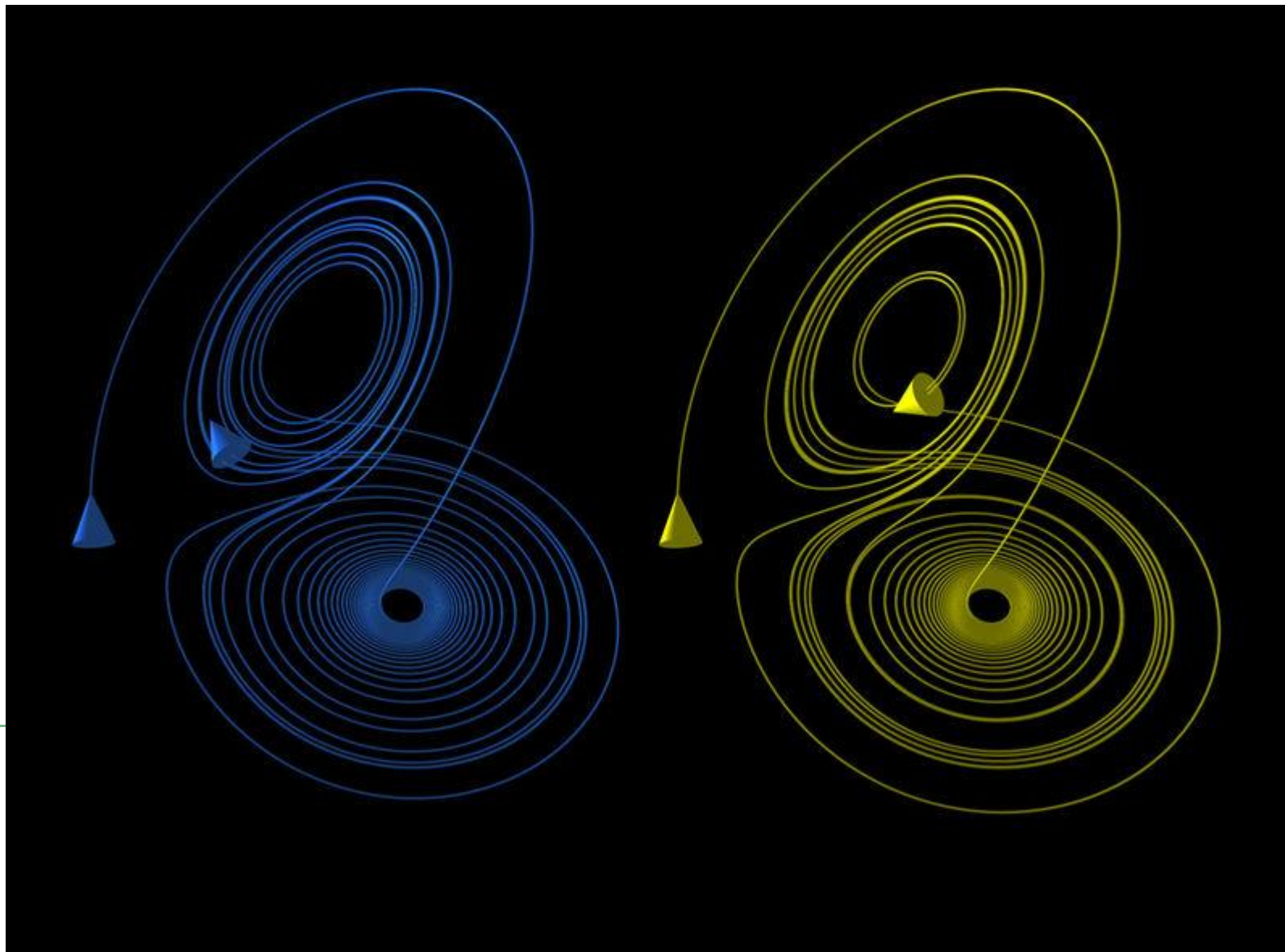


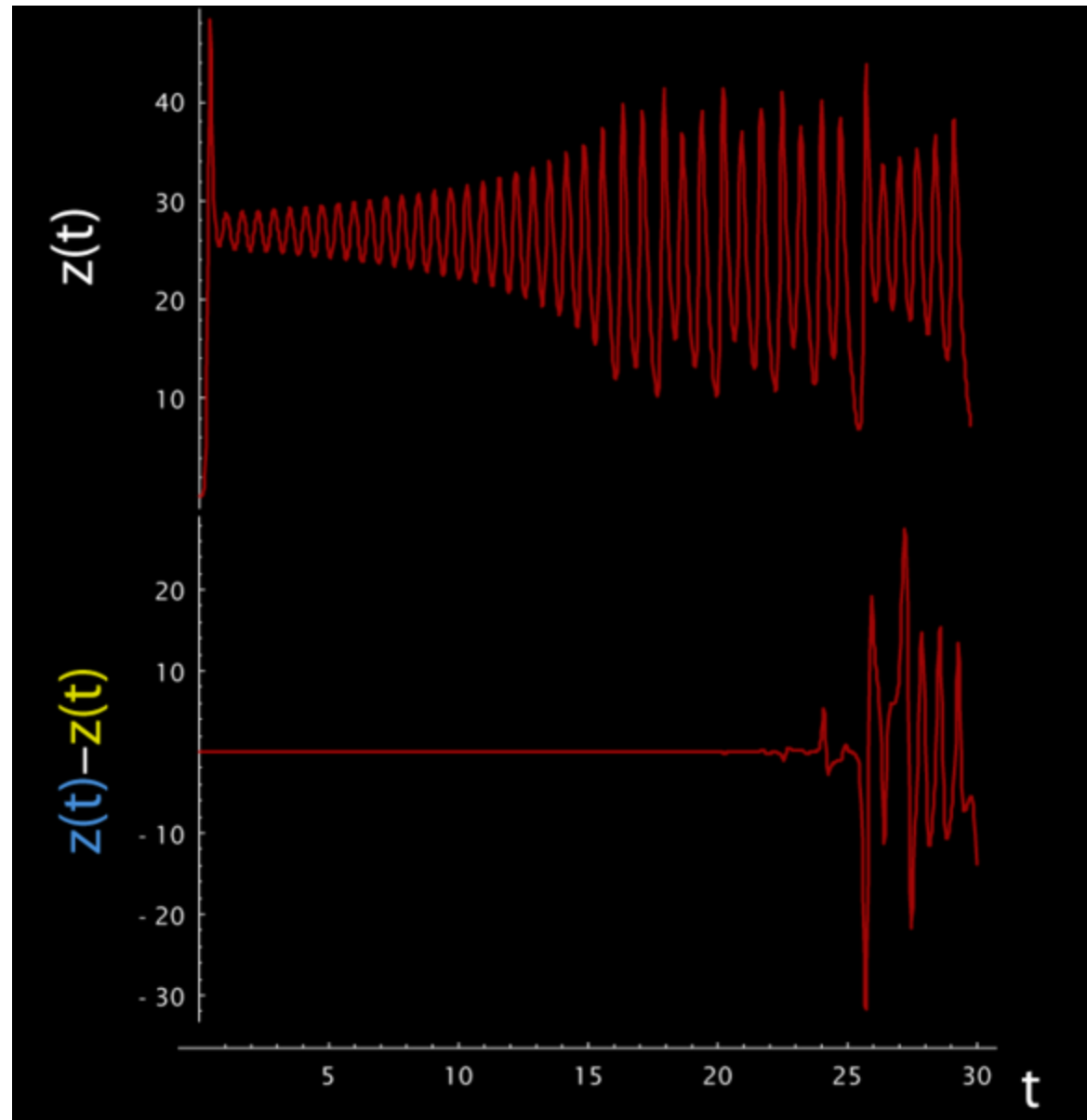
Possible within the laws of physics !!

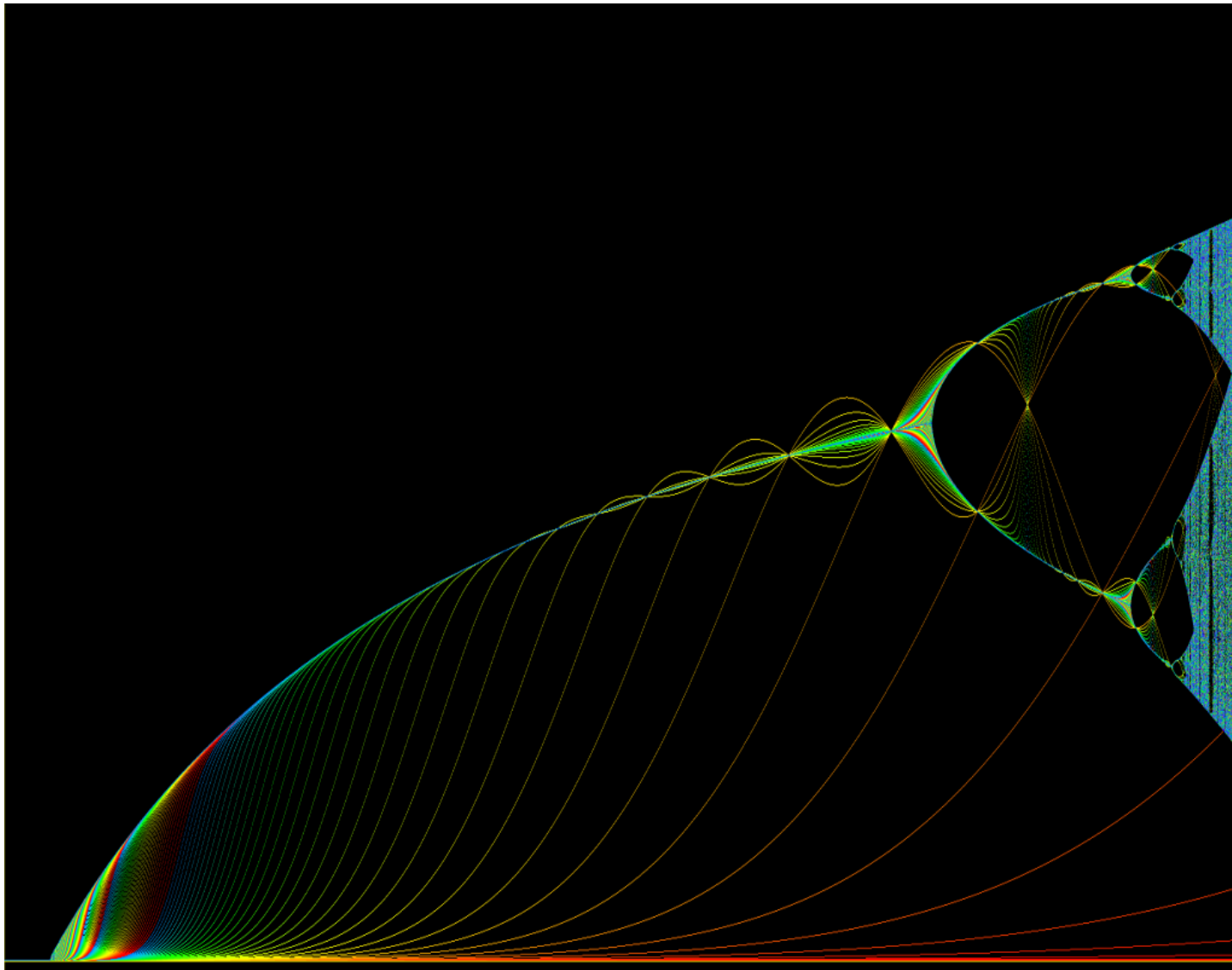
Maybe not so likely !



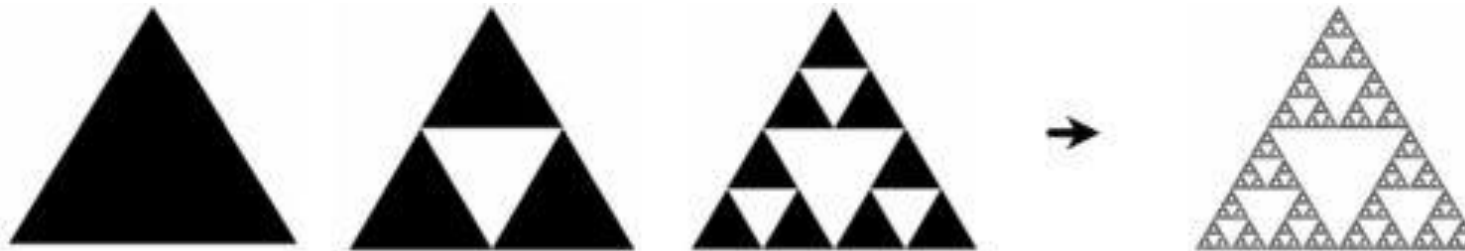
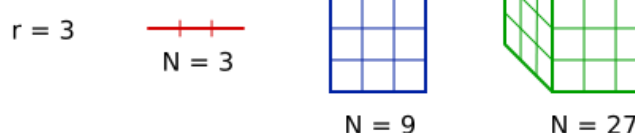
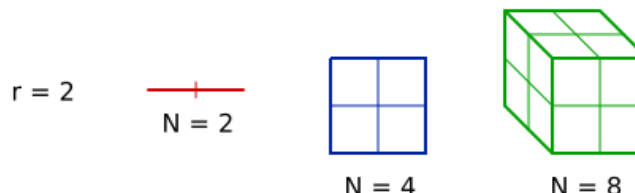
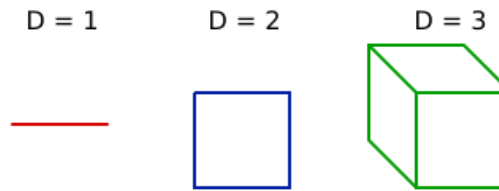
The Butterfly Effect (in Lorenz attractor)





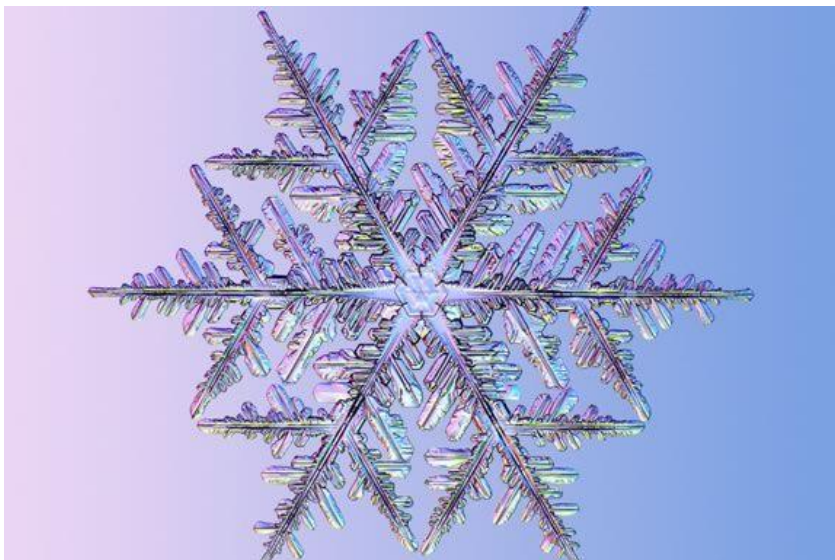


Fractals: Non-integer Dimensions



$$D = \lim_{\epsilon \rightarrow 0} \frac{\log N(\epsilon)}{\log \left(\frac{1}{\epsilon} \right)} = \lim_{k \rightarrow \infty} \frac{\log 3^k}{\log 2^k} = \frac{\log 3}{\log 2} \approx 1.585$$

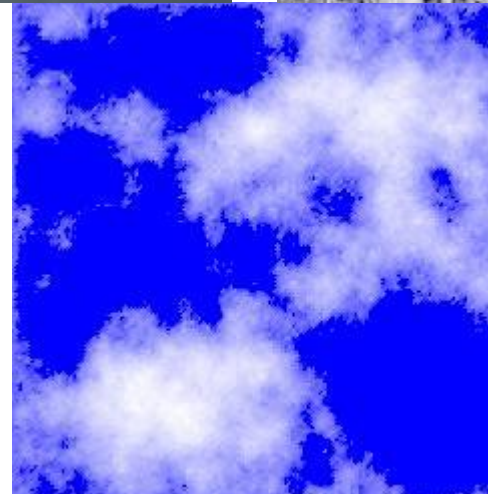




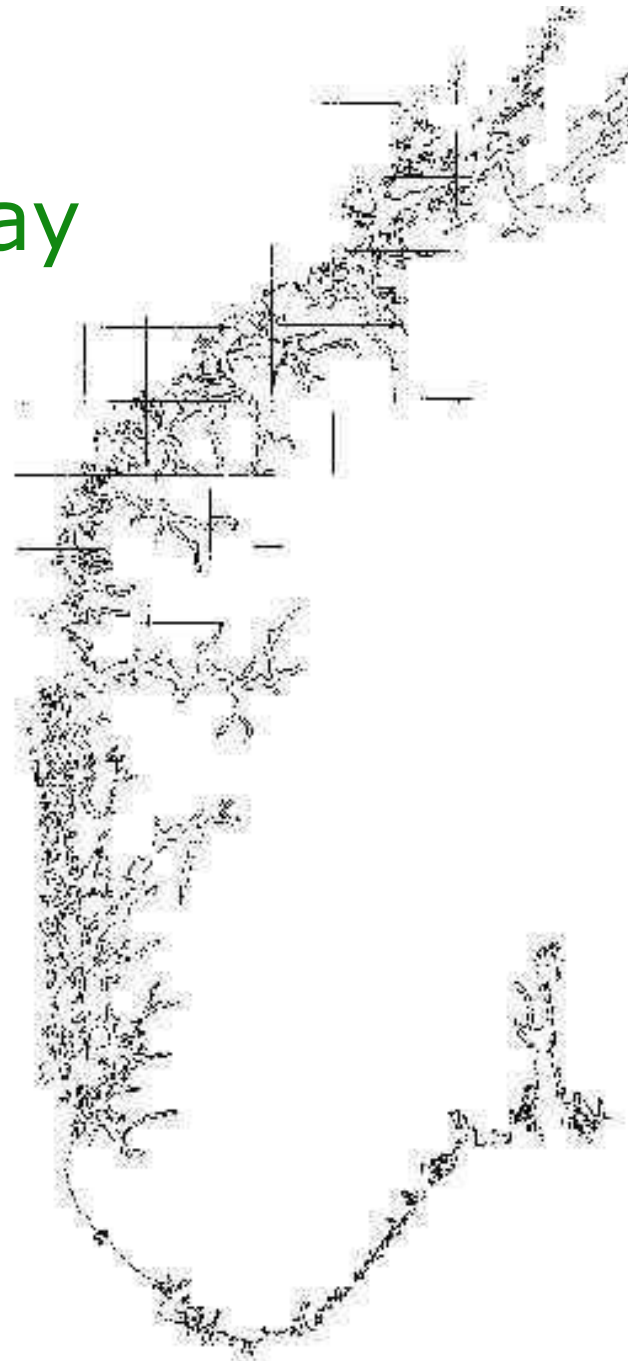
Snowflakes are
fractals !



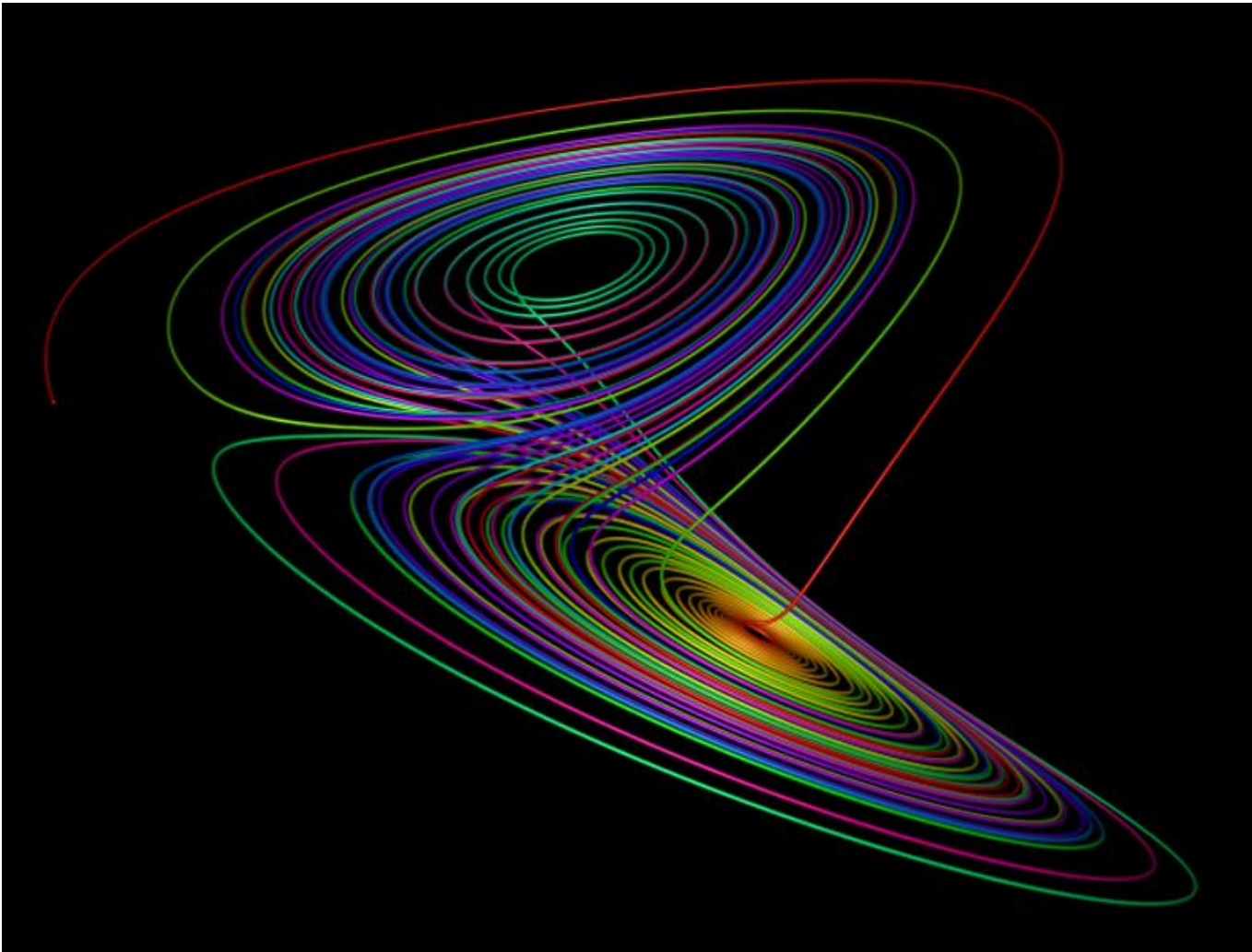
Clouds are fractals !



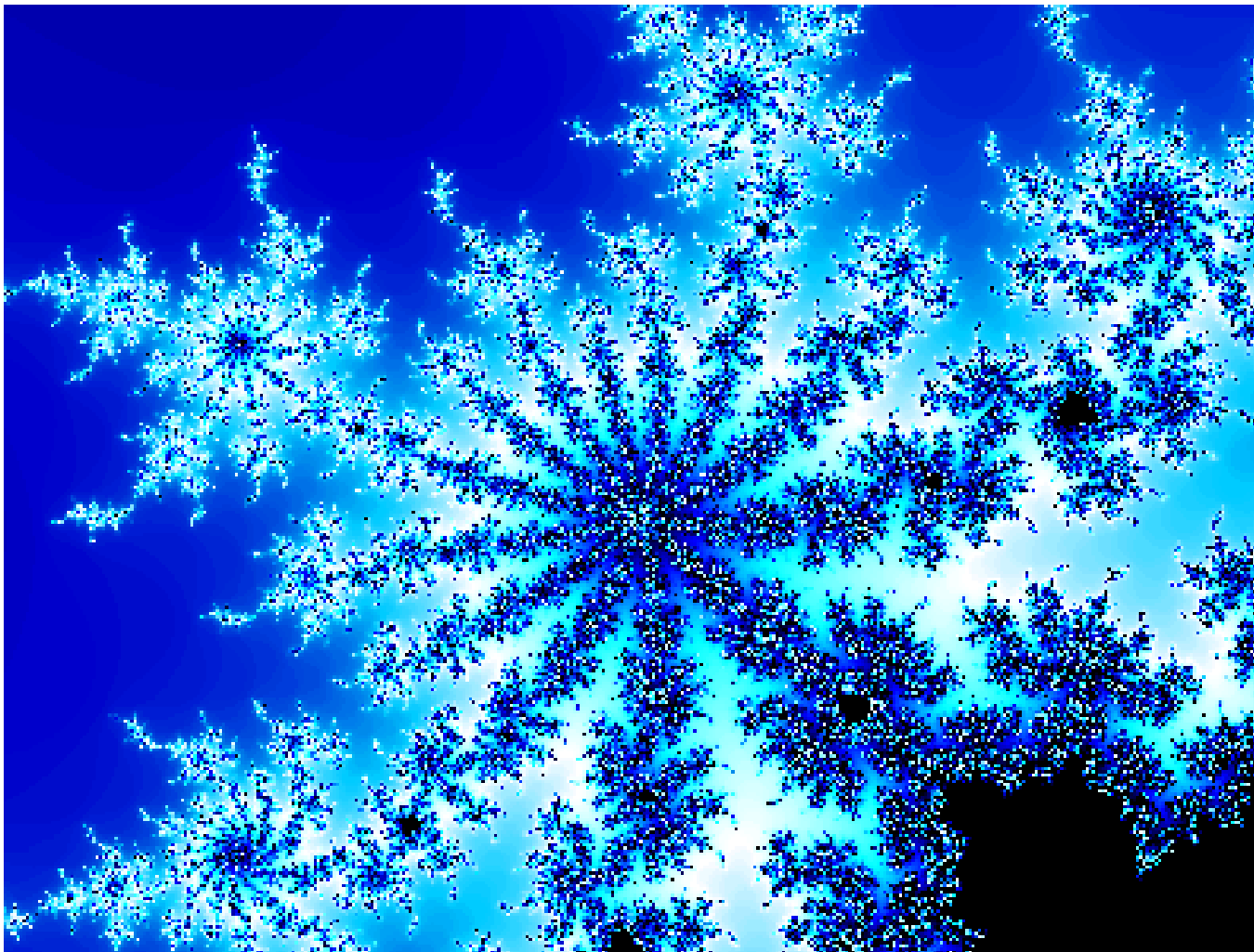
The coast of Norway is a fractal !



Chaotic systems are fractals !

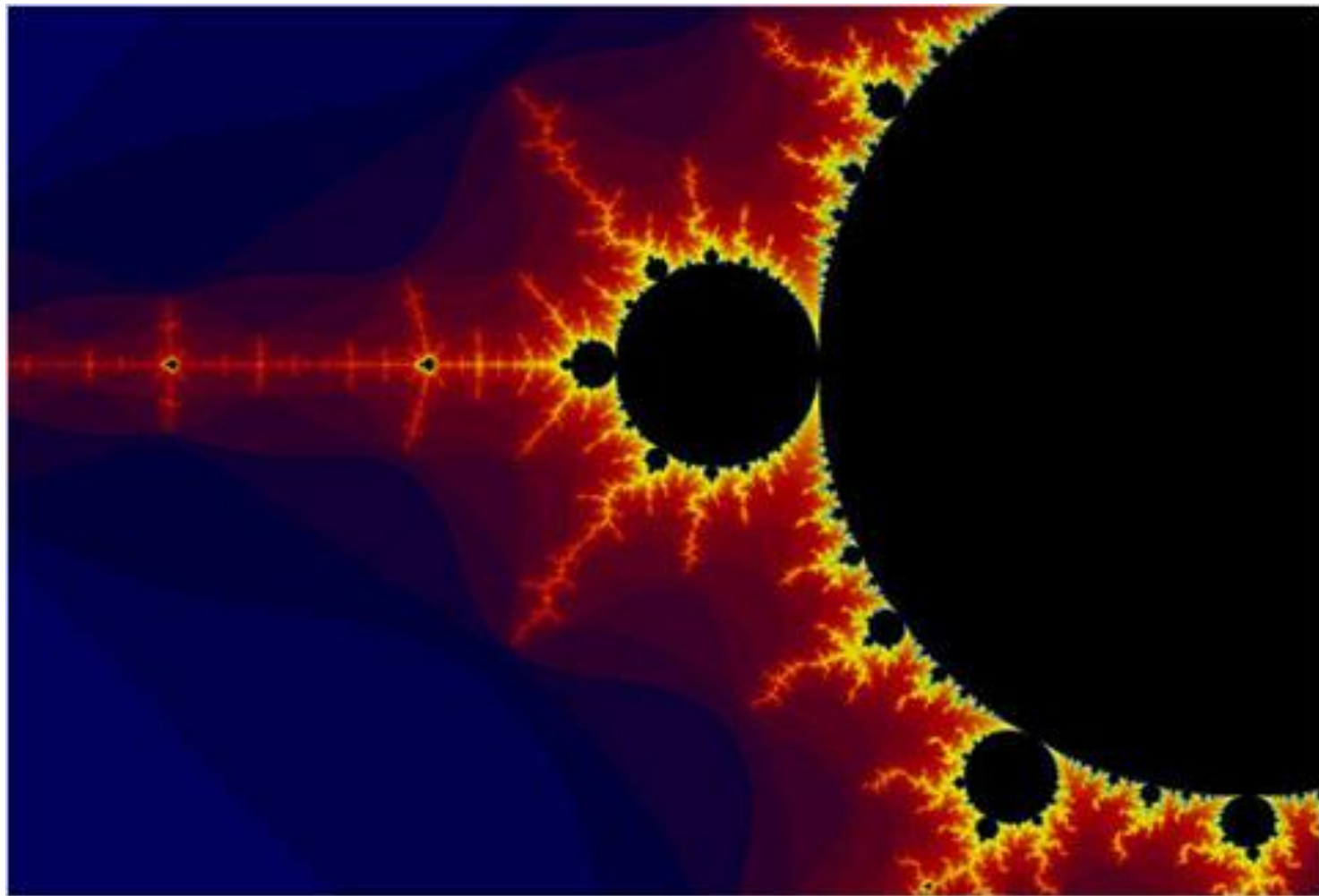


Mathematical fractals !



Julia set





Mandelbrot set



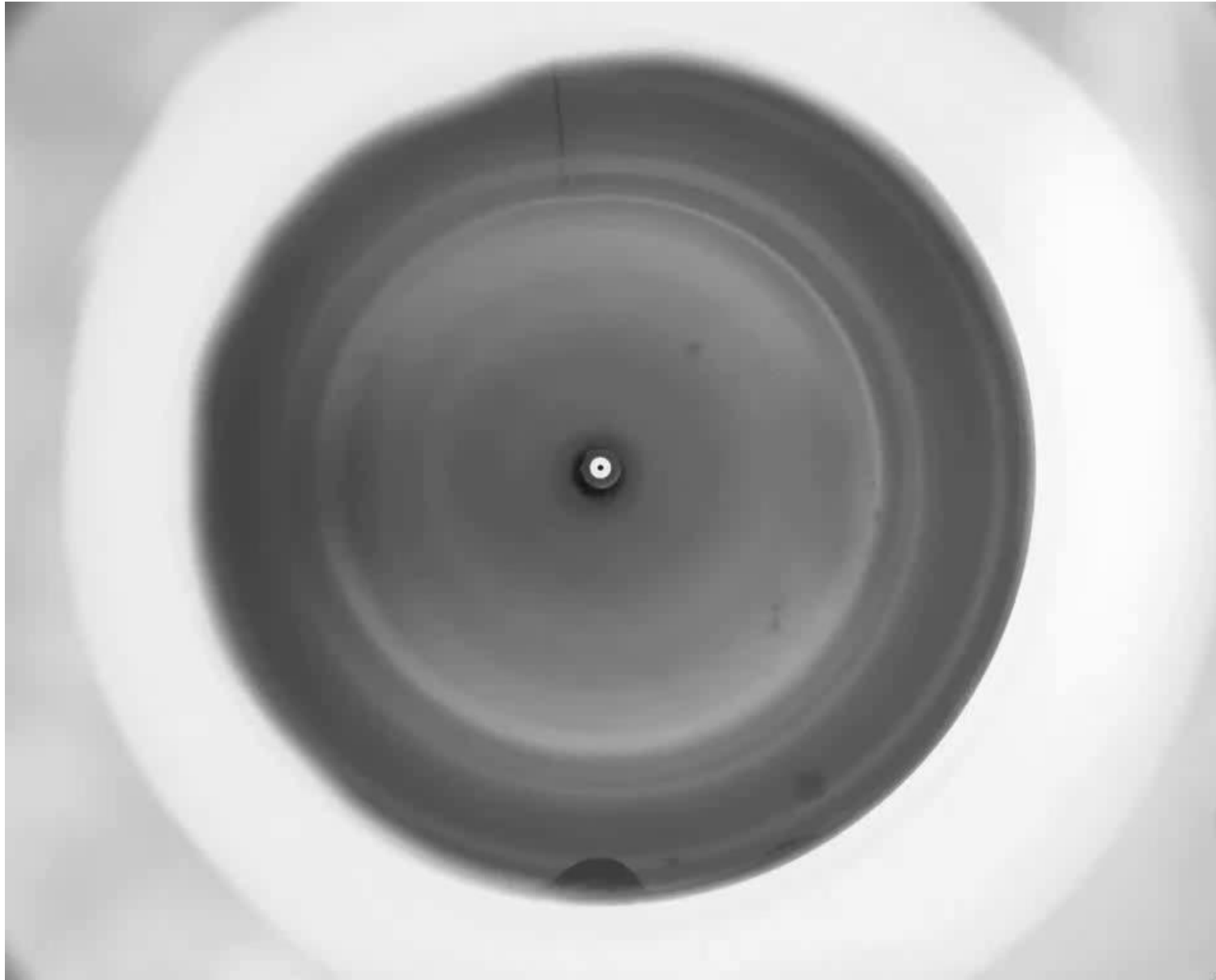
Viscous finger: Important for oil recovery.

Water into oil



Fractals and oil: Niels Bohr Intsitute and Oslo University!





Swinney
Mathiesen

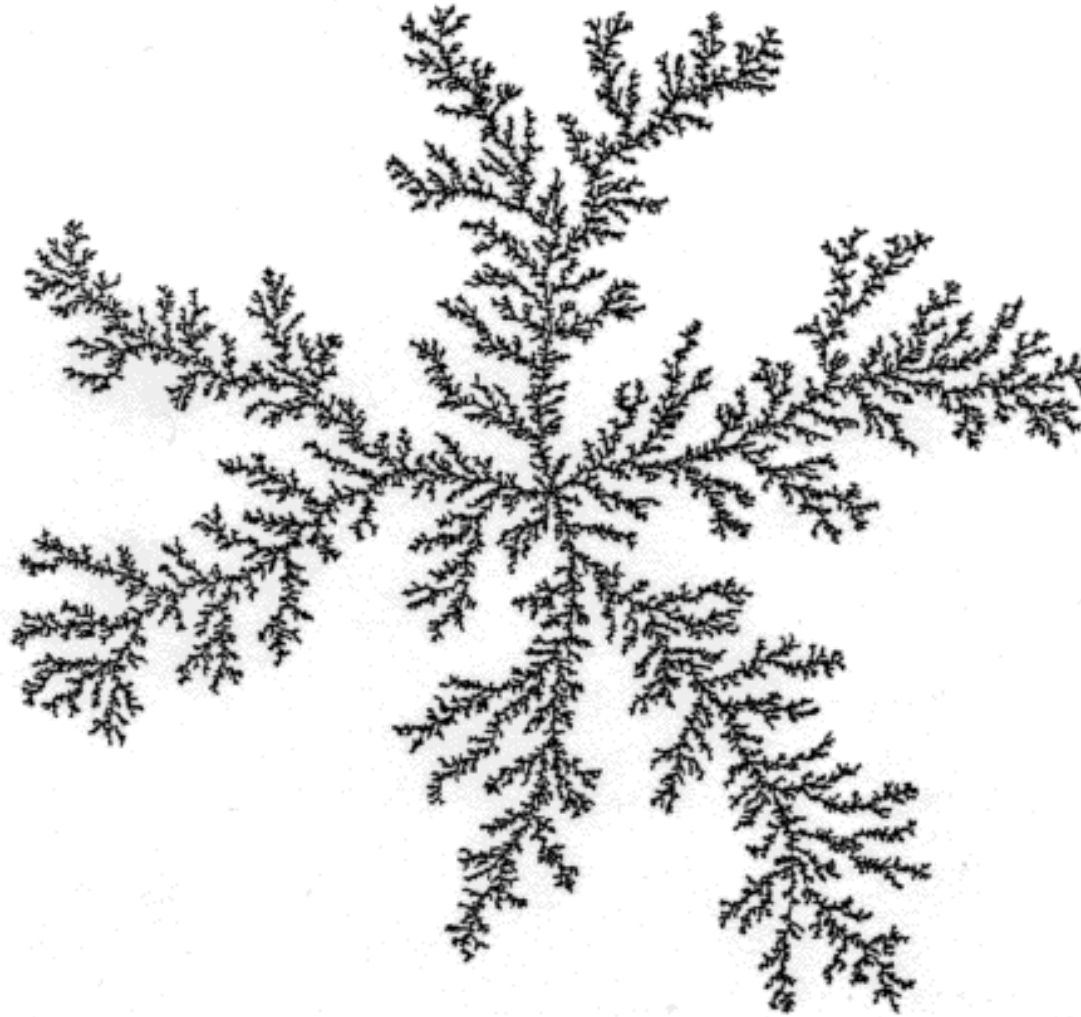




Patterns and flow in frictional fluid dynamics

Complexity group, University of Oslo

Model for fractal fingers (DLA):



Self-similar on all scales !

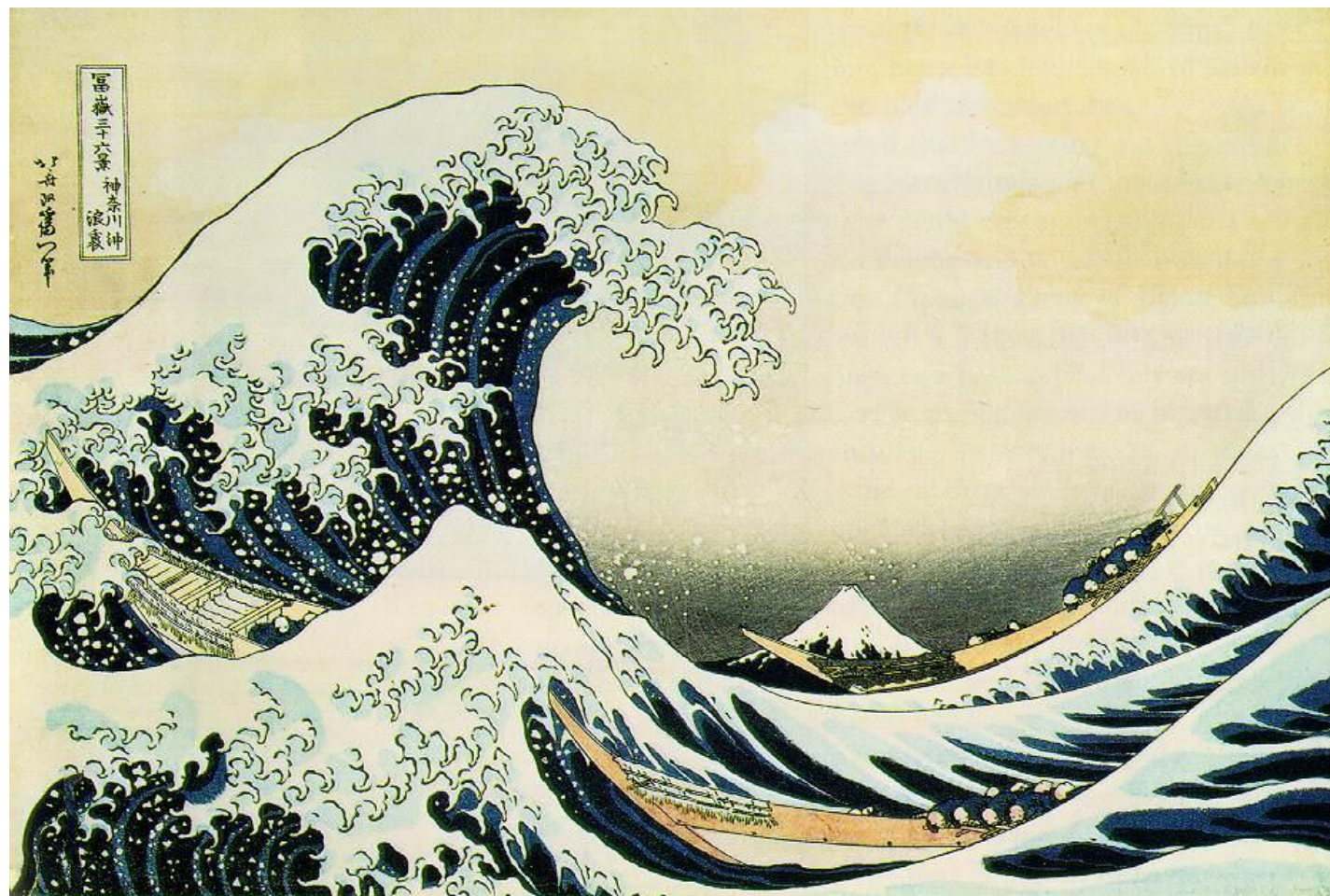


The atmosphere is turbulent, fractal and chaotic !



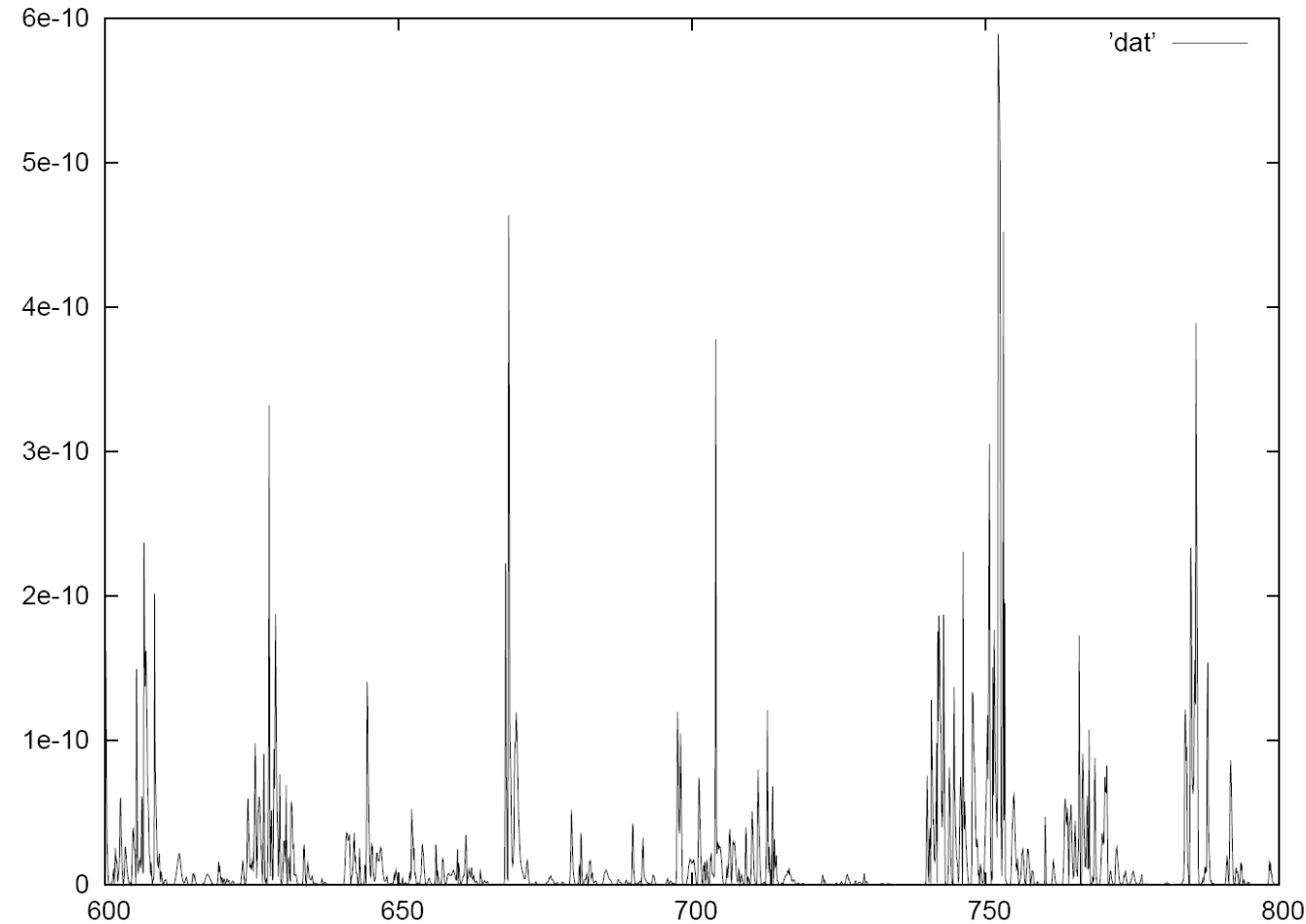
Boiling water !





Energy
dissipation

νu_{15}^2



Turbulence → Intermittency/avalanches !





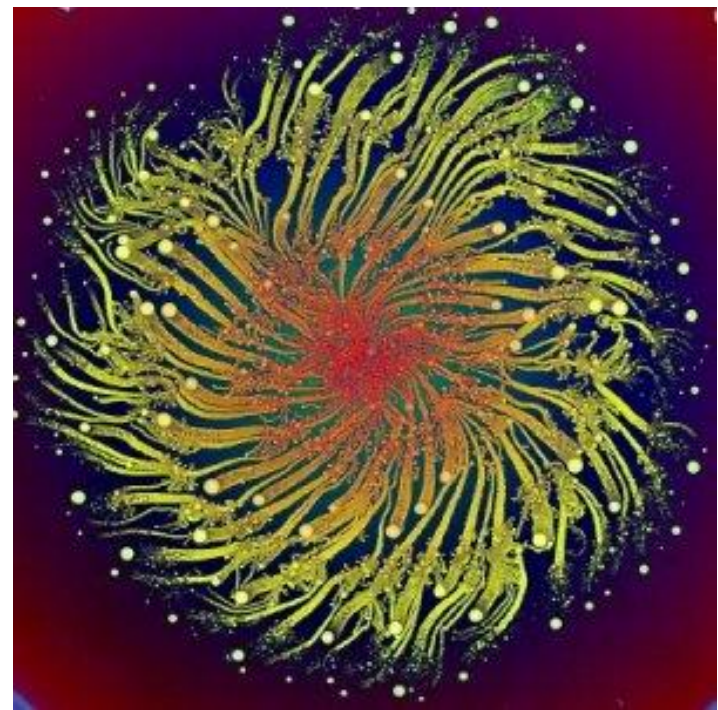
Dynamics in Complex Systems

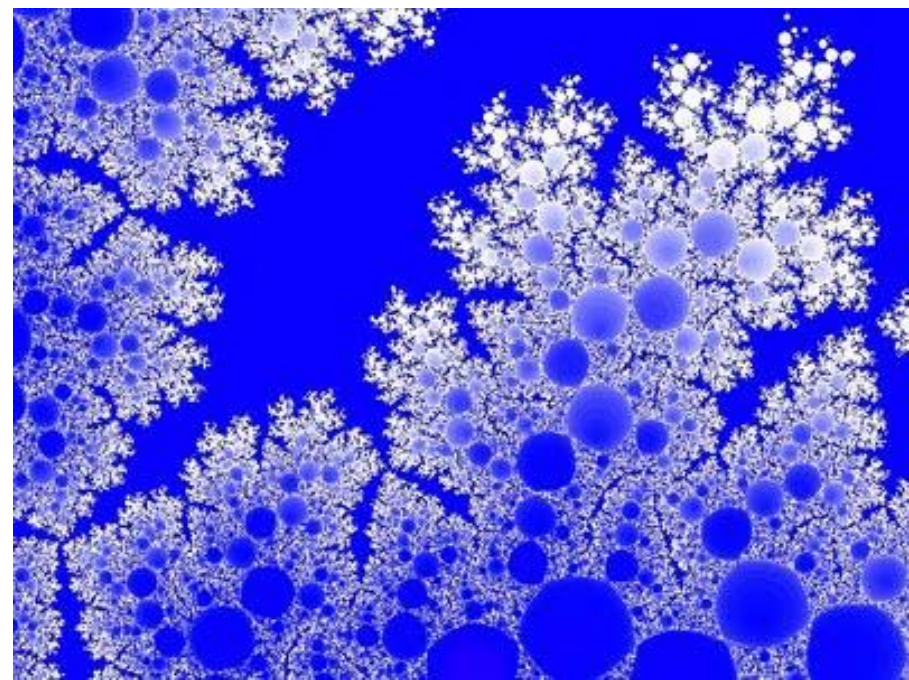
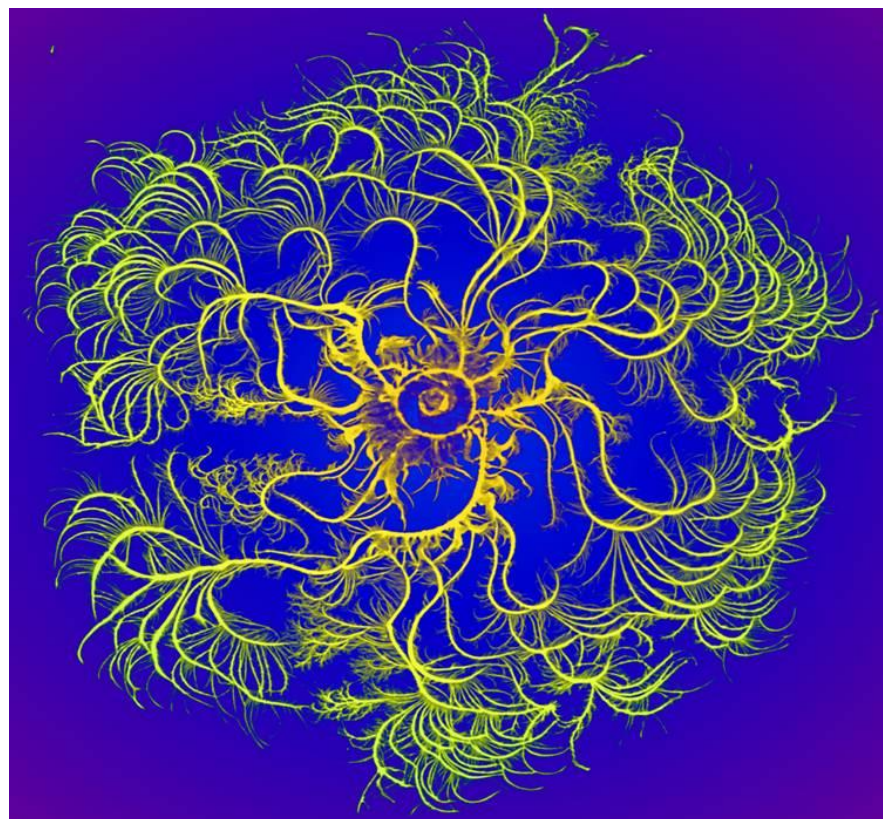
Avalanches !!

Avalanches have a high probability – Non Gaussian !

Paradigm model: Per Bak sandpile

Bacteria can grow as fractals

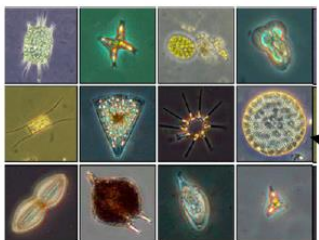




Phytoplankton blooms at high Reynolds number in the Norwegian Sea and near Iceland



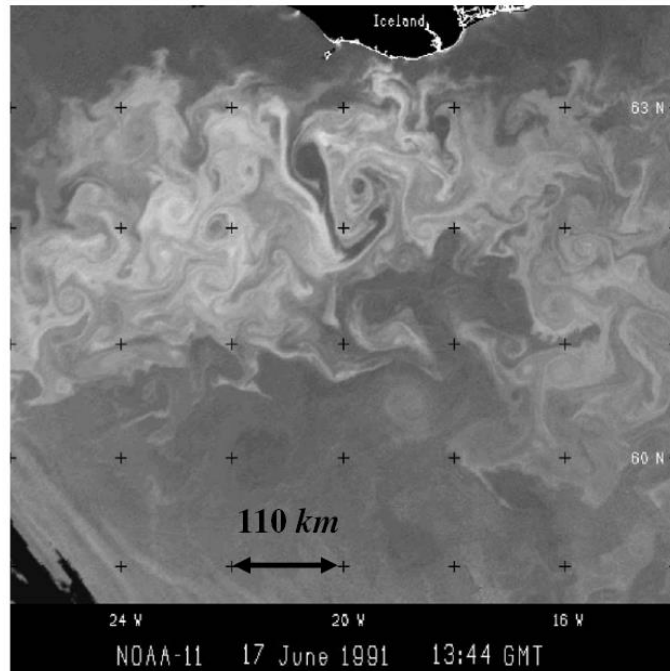
<http://visibleearth.nasa.gov/cgi-bin/viewrecord?5278>
see also, Tel. et al. Phys. Rep. **413**, 91 (2005).



mixing layer $\approx 25\text{-}100$ m.

Phytoplankton
(see also zooplankton & bacterioplankton)

http://earthobservatory.nasa.gov/Experiments/ICE/Channel_Islands/



A. P. Martin, Prog. Oceanography **57**, 125 (2003)

$$\text{Re} = LU / \nu = 10^8 - 10^9$$

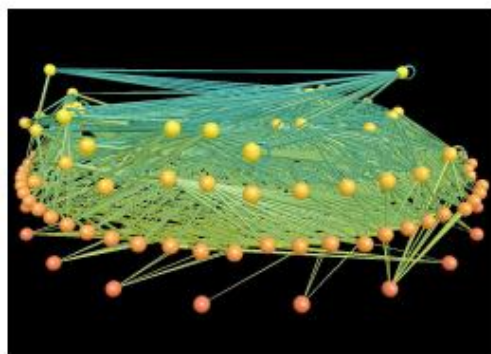
Large eddy turnover time ≈ 50 days

Small eddy turnover time ≈ 5 minutes

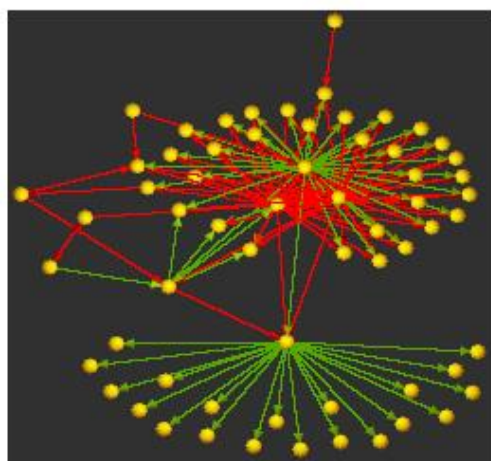
Plankton doubling time ≈ 12 hours



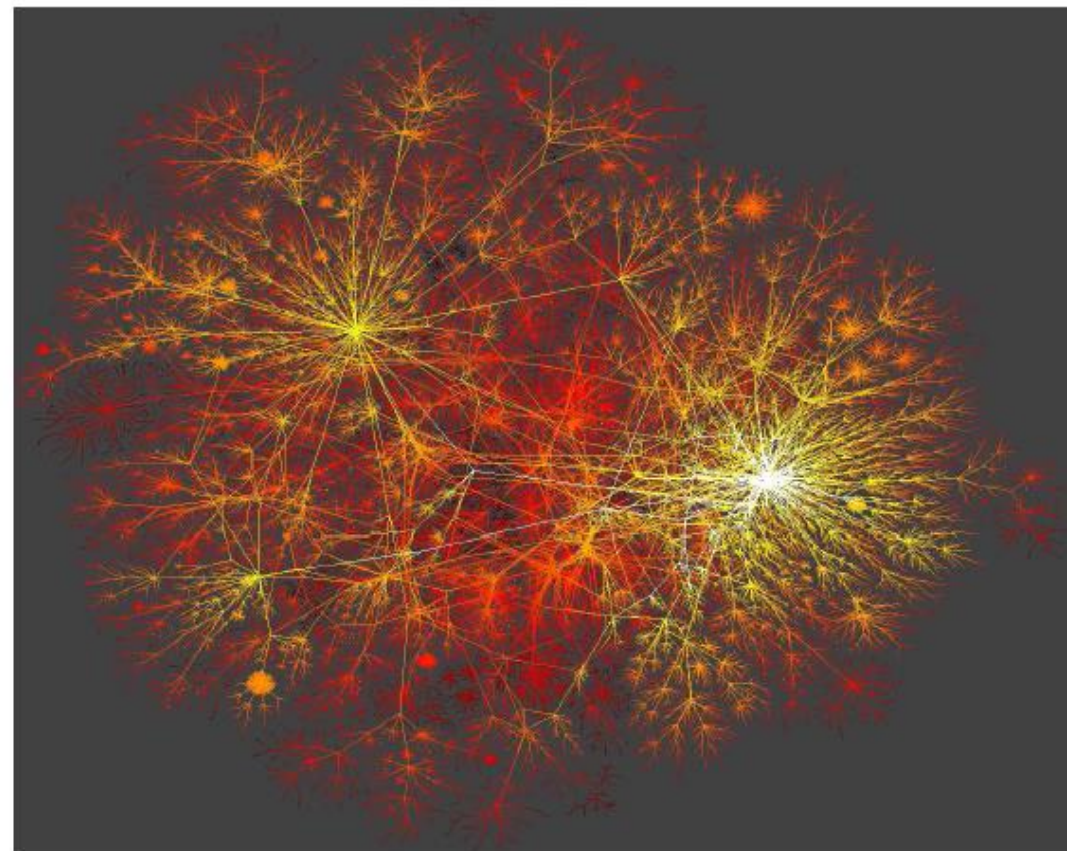
Networks: Fractal structures !



Freshwater food web.
N. Martinez, R. Williams



Protein regulation in λ

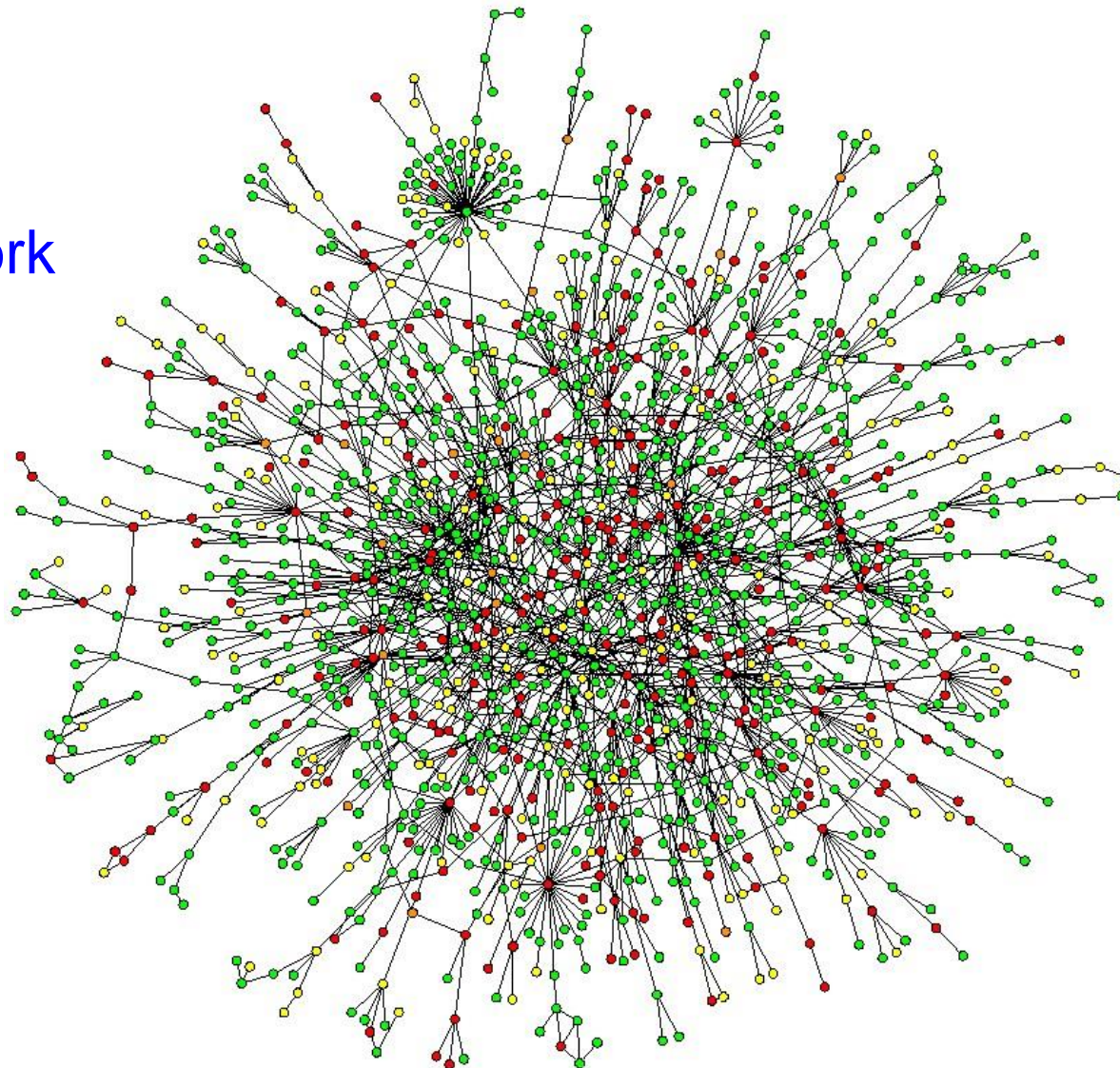


Internet
K. C. Claffy

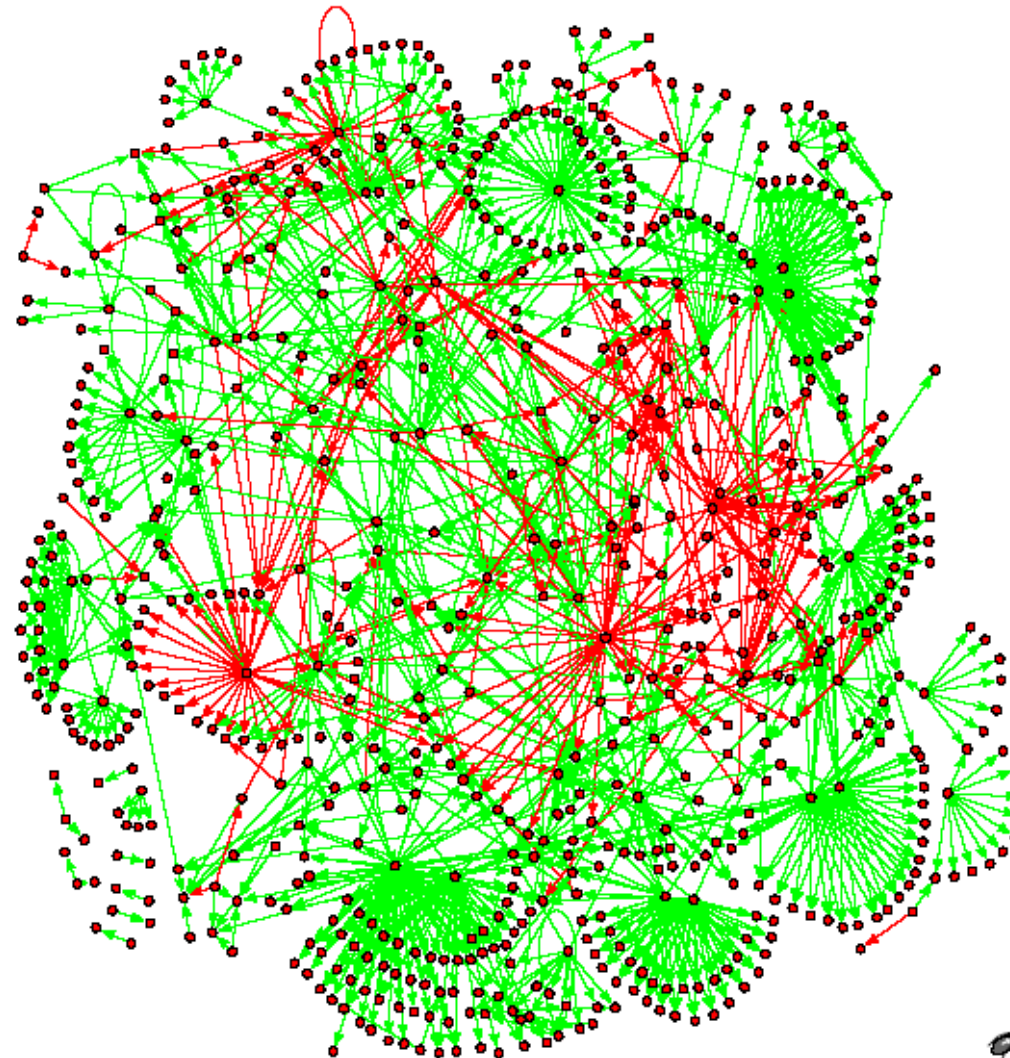


This is how yeast looks !

Protein network



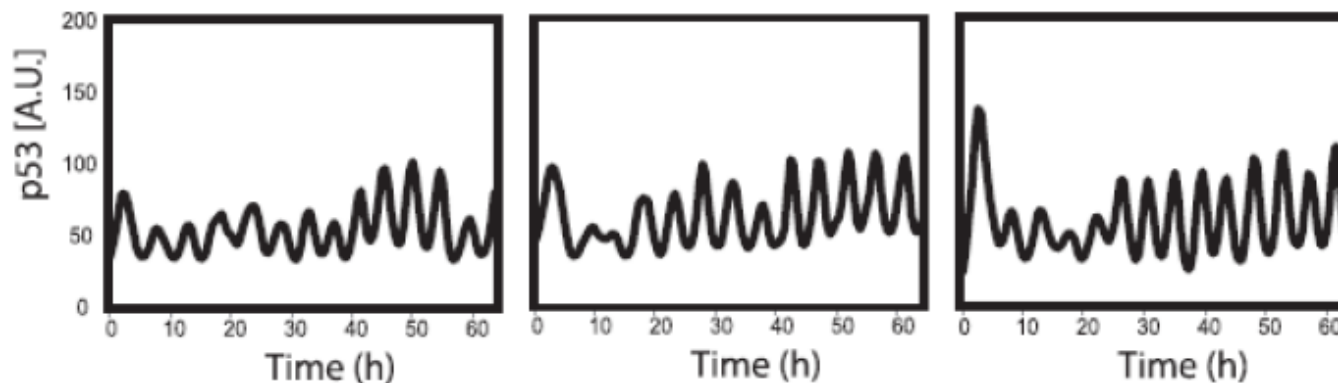
Another 'fractal' picture of yeast !



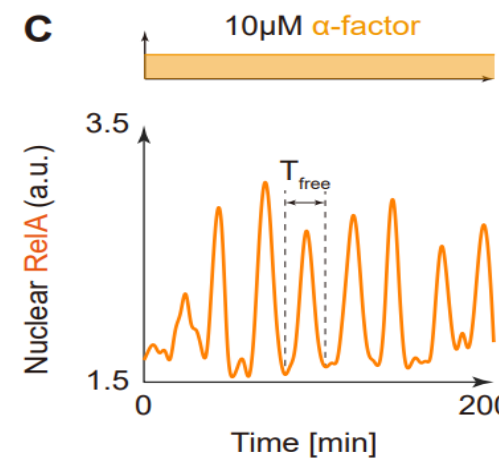
Pajek



Gamma radiation on human (MCF7) cancer cells: p53 oscillate (Lahav, Harvard)

DSBs

Alpha-factor on yeast cells: NF- κ B oscillate (Beijing/Shenzhen, Ping Wei)



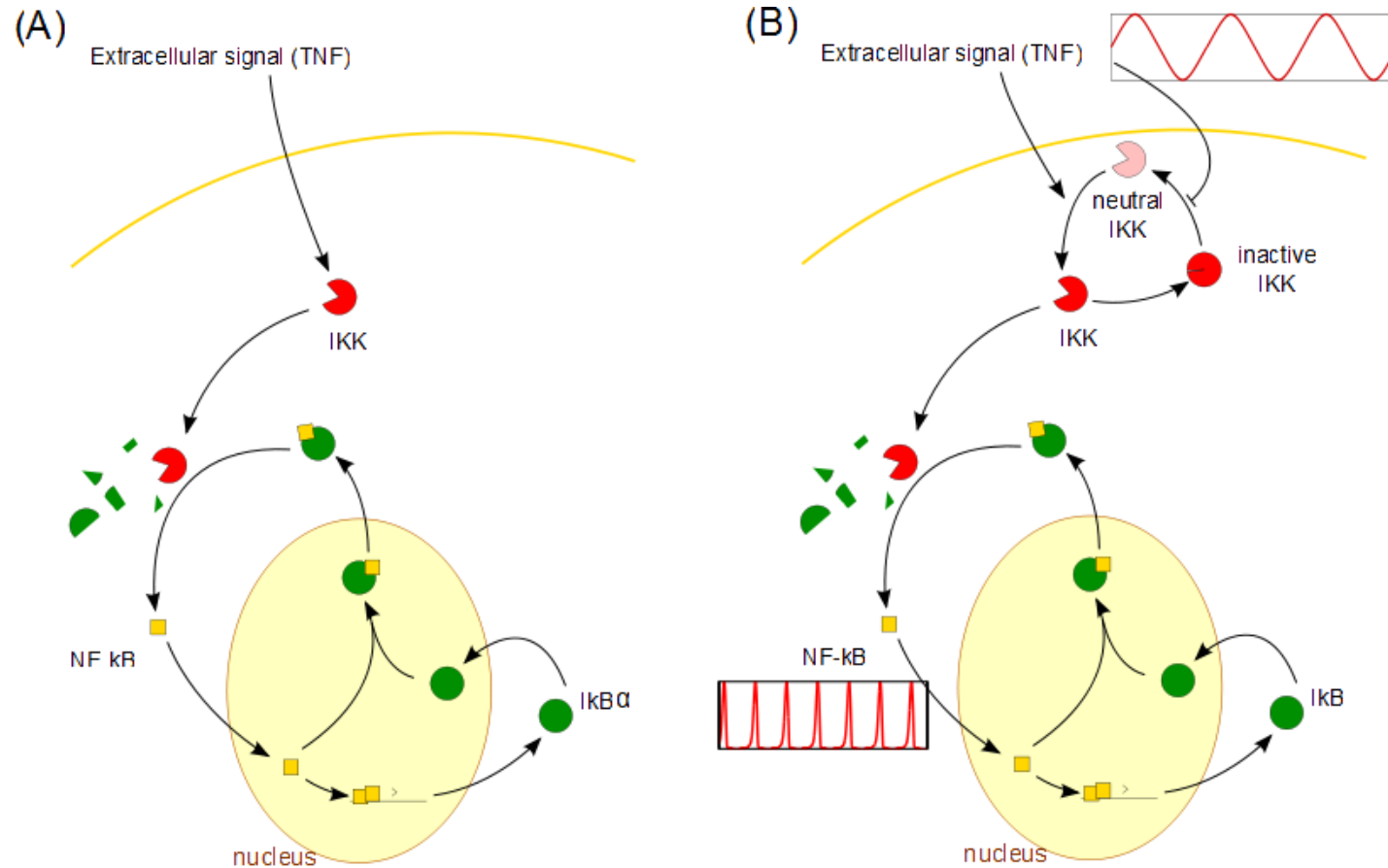
Our research:

Can we control and understand it?

Can it be used for gene regulation and control and DNA repair?



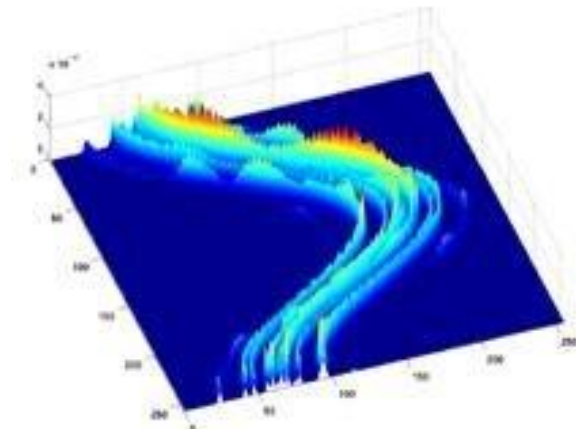
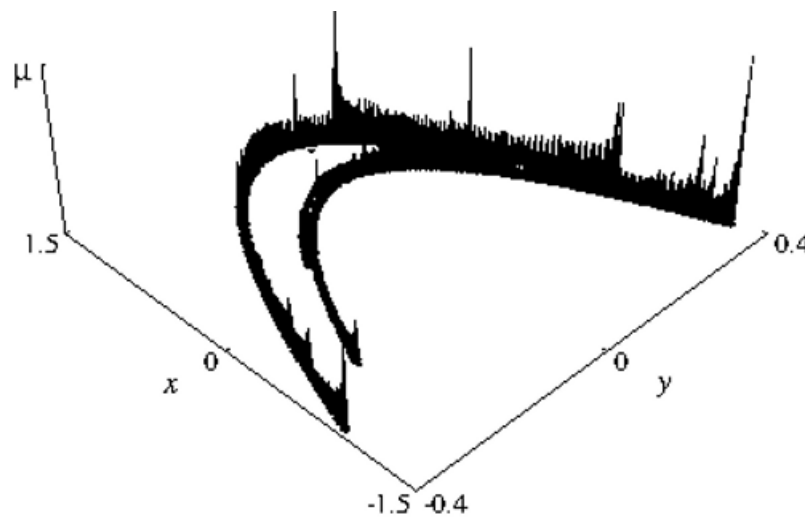
Externally 'forced' NF-κB system



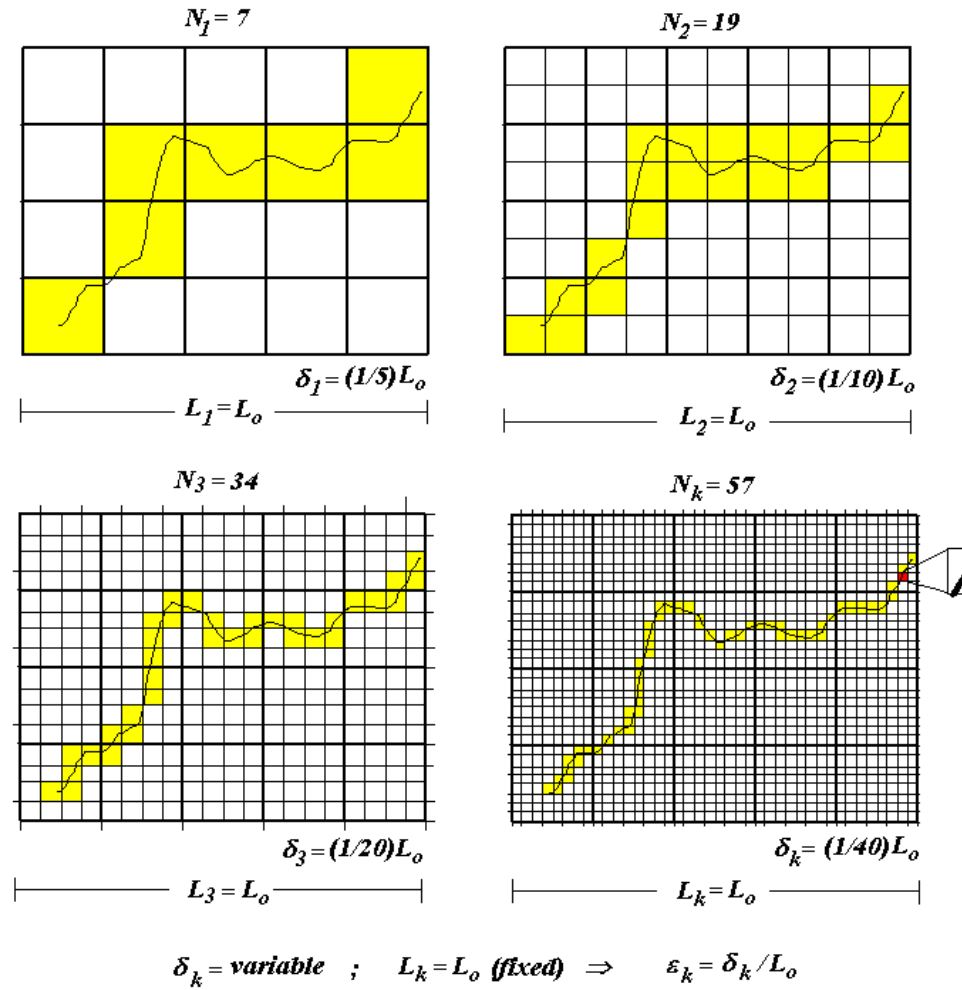
(S. Krishna, MHJ)



Back to fractals: If there is a density on (a measure): Multifractal



Cover a fractal with boxes (smaller and smaller)!



i'th box size l_i and density in box p_i :

Pointwise dimension α : $p_i \sim l_i^\alpha$

$$p_i = \int_{i\text{th box}} d\mu(\mathbf{x}) .$$

In many nonlinear behavior is richer and more critical phenomena. If a saying that

$$p_i^q \sim l_i^{\alpha q} ,$$

then α [roughly equivalent on a range of values, corresponds to the measure. In particular pieces of size l , we suggest takes on a value between form

$$d\alpha' \rho(\alpha') l^{-f(\alpha')} ,$$

We have an infinity of pointwise dimensions α !

$$D_q = \lim_{l \rightarrow 0} \left[\frac{1}{q-1} \frac{\ln \chi(q)}{\ln l} \right] ,$$

where

$$\chi(q) = \sum_i p_i^q .$$

D_0 is just the fractal dimension of the surface, while D_1 is the information dimension correlation dimension.¹⁴

As q is varied in Eq. (1.7), different scaling associated with different scaling indices obtain. Substituting Eqs. (1.4) and (1.5) obtain

$$\chi(q) = \int d\alpha' \rho(\alpha') l^{-f(\alpha')} l^{q\alpha'} .$$

Since l is very small, the integral in Eq. dominated by the value of α' which makes $f(\alpha')$ least, provided that $\rho(\alpha')$ is nonzero. Thus $\alpha(q)$, which is defined by the extremal condition

$$\frac{d}{d\alpha'} [q\alpha' - f(\alpha')] \Big|_{\alpha'=\alpha(q)} = 0 .$$

We also have

$$\frac{d^2}{d(\alpha')^2} [q\alpha' - f(\alpha')] \Big|_{\alpha'=\alpha(q)} > 0 ,$$

so that

$$f'(\alpha(q)) = q ,$$

$$f''(\alpha(q)) < 0 .$$



Legendre transform!

$$\alpha(q) = d\tau(q)/dq ,$$

$$f(q) = qd\tau/dq - \tau(q) .$$

$$\tau(q) \quad \longleftrightarrow \quad f(\alpha)$$

We define $\tau(q) = (q-1)D_q$



Two scale cantor set:

Sizes l_1, l_2 , densities p_1, p_2 !

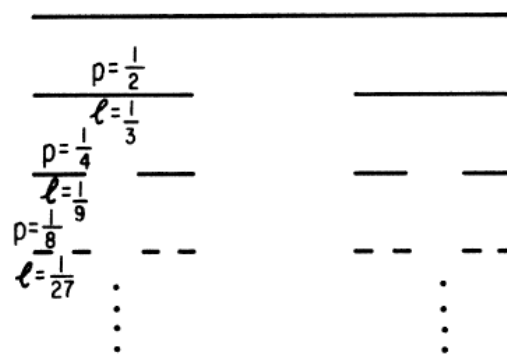


FIG. 1. The construction of the uniform Cantor set. At each stage of the construction the central third of each segment is removed from the set. Each segment has measure $p_0=(\frac{1}{3})^n$ and scale $l_0=(\frac{1}{3})^n$, where n is the number of generations.

3. Uniform Cantor set

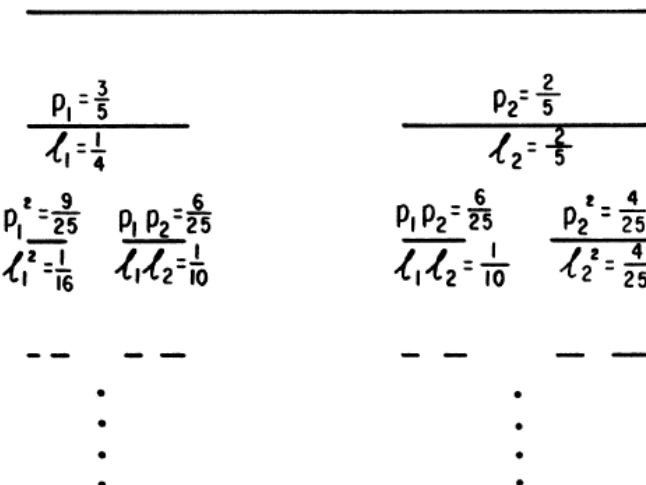


FIG. 2. A Cantor-set construction with two rescalings $l_1=0.25$ and $l_2=0.4$ and respective measure rescalings $p_1=0.6$ and $p_2=0.4$. The division of the set continues self-similarly.



Generalized partition sum:

$$\Gamma(q, \tau, l_2^n) = \left[\frac{p_1^q}{l_1^\tau} + \frac{p_2^q}{l_2^\tau} \right]^n = 1 \quad (2.24)$$

results in a τ that does not depend on n . The value of τ depends, however, on q . In Fig. 3 we show $D_q = \tau(q)/(q - 1)$ as a function of q , as obtained numerically by solving Eq. (2.24). To further understand this curve, we can examine the quantity $\Gamma(l_2^n)$ for this case explicitly:

$$\Gamma(q, \tau, l_2^n) = \sum_m \binom{n}{m} p_1^{mq} p_2^{(n-m)q} (l_1^m l_2^{n-m})^{-\tau} = 1 . \quad (2.25)$$

We expect that in the limit $n \rightarrow \infty$ the largest term in this sum should dominate. To find the largest term we compute

$$\frac{\partial \ln \Gamma(l_2^n)}{\partial m} = 0 . \quad (2.26)$$

Using the Stirling approximation, we find that Eq. (2.26) is equivalent to

$$\tau = \frac{\ln(n/m - 1) + q \ln(p_1/p_2)}{\ln(l_1/l_2)} . \quad (2.27)$$



Multifractal $f(\alpha)$ spectrum of two scale cantor set:

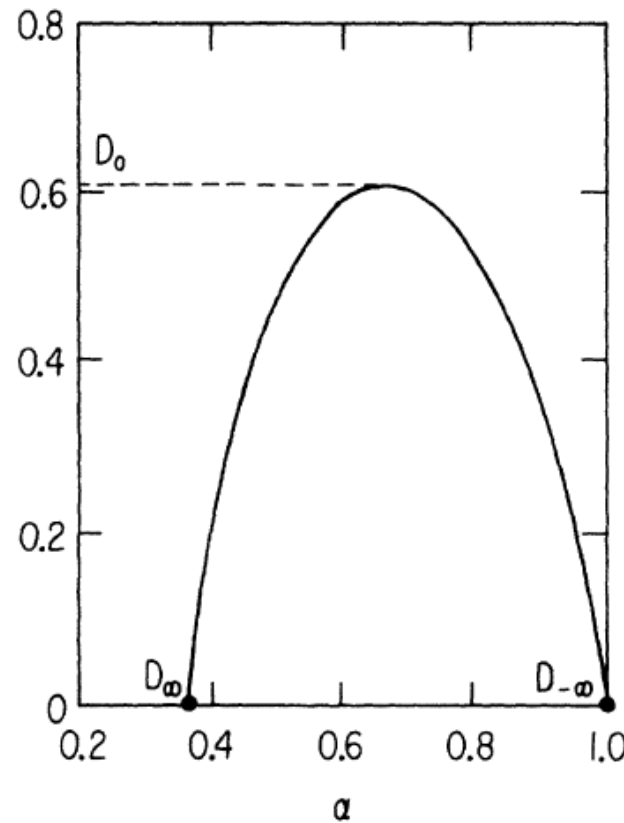
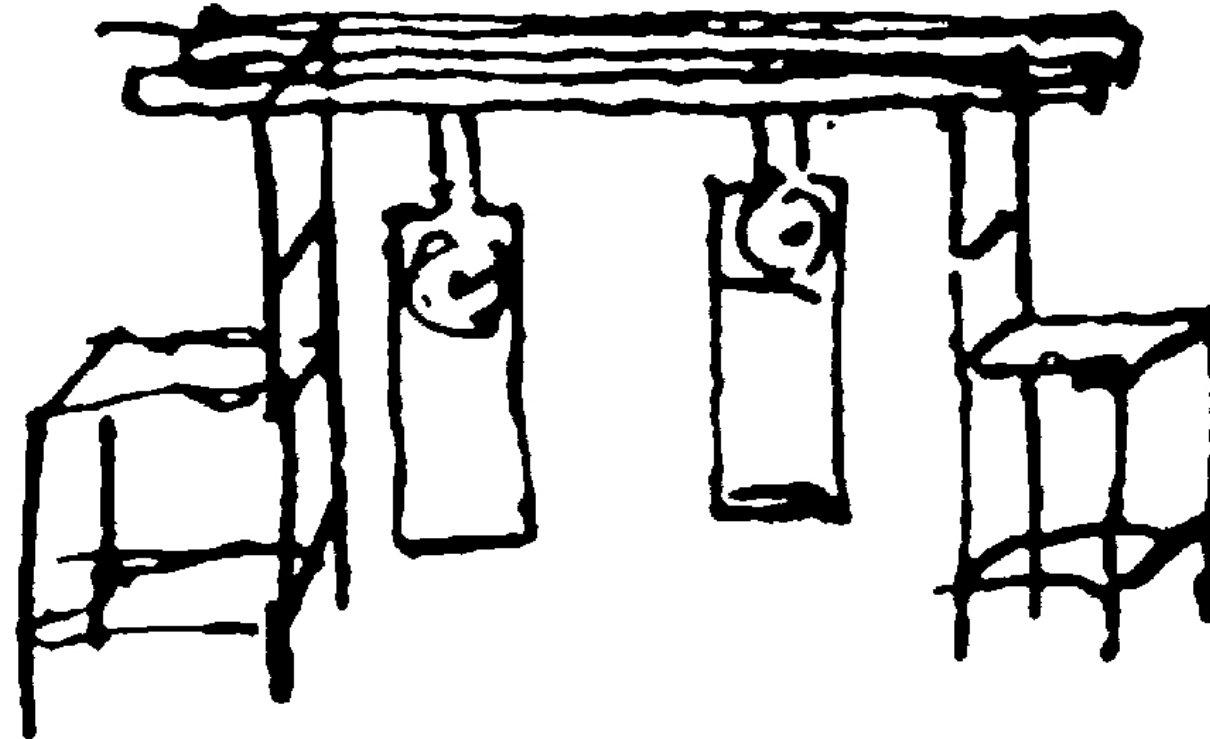


FIG. 4. The plot of f vs α for the set in Fig. 2. Note that $f=0$ corresponds to α values $D_{-\infty} = \ln(0.4)/\ln(0.4) = 1.0$ and $D_\infty = \ln(0.6)/\ln(0.25) = 0.3684$.



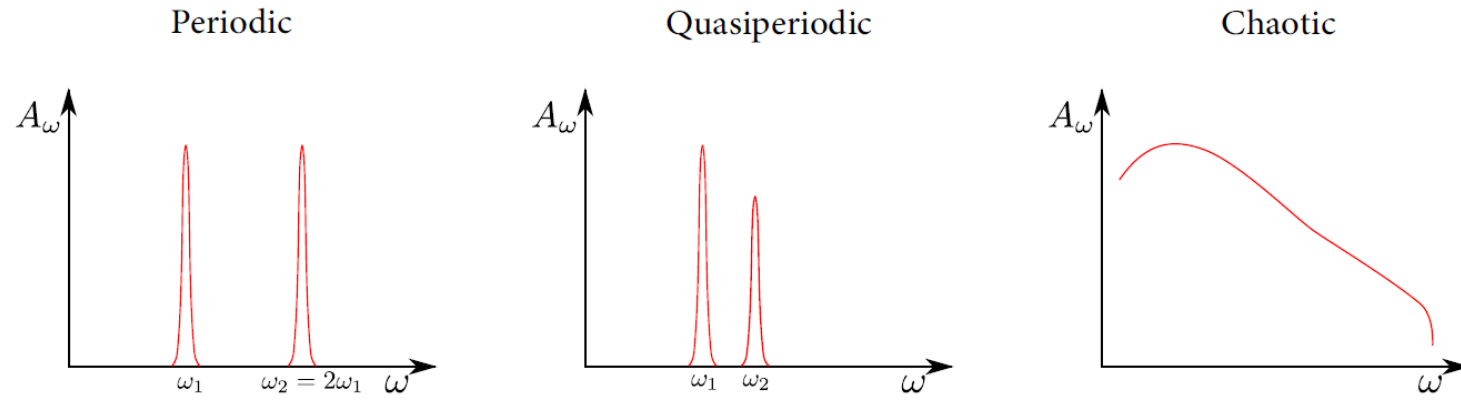
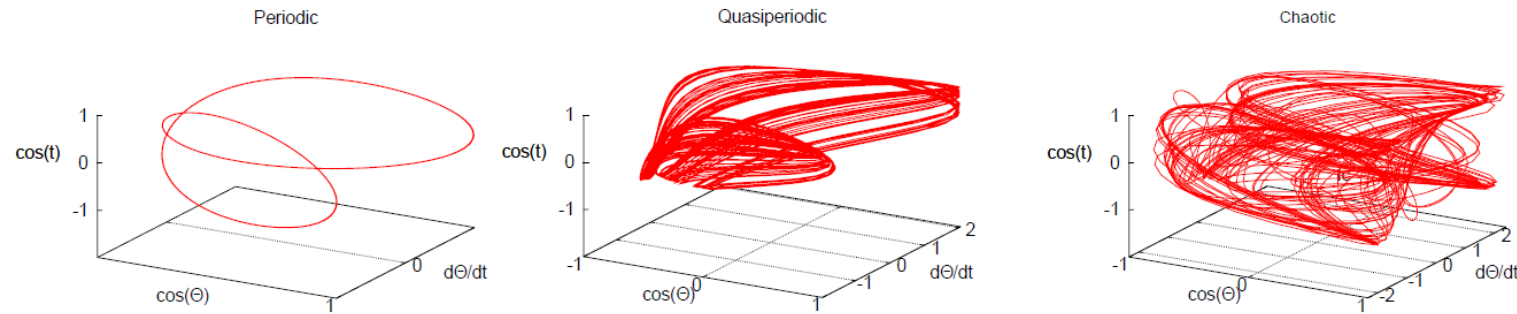
Synchronization of two oscillators



Huygens' clocks 1665

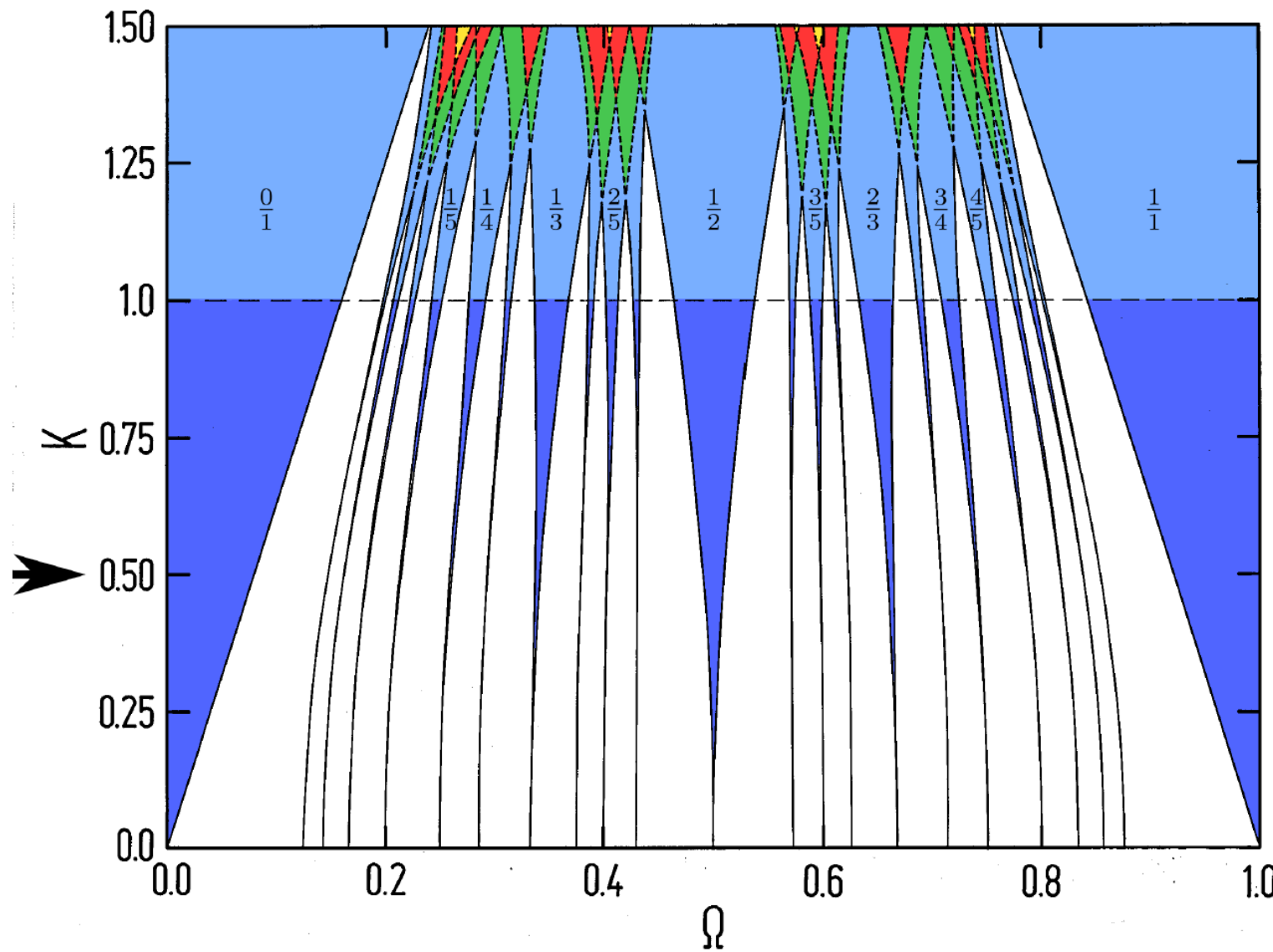


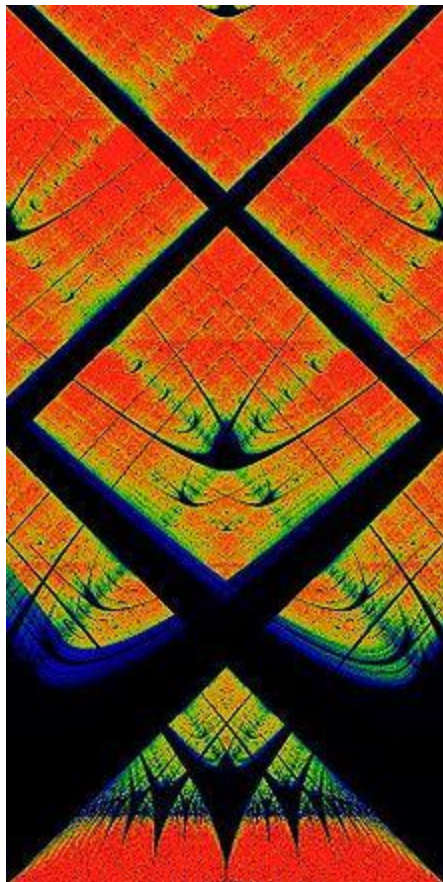
Three different non-linear dynamics



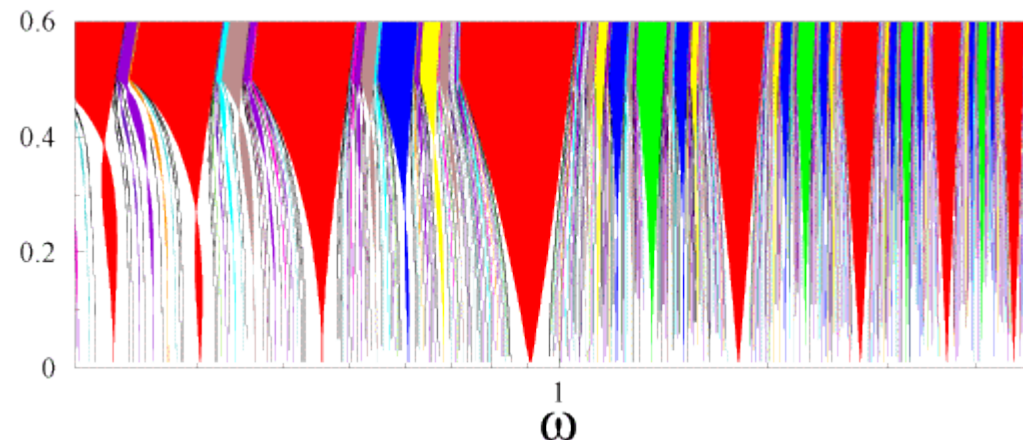
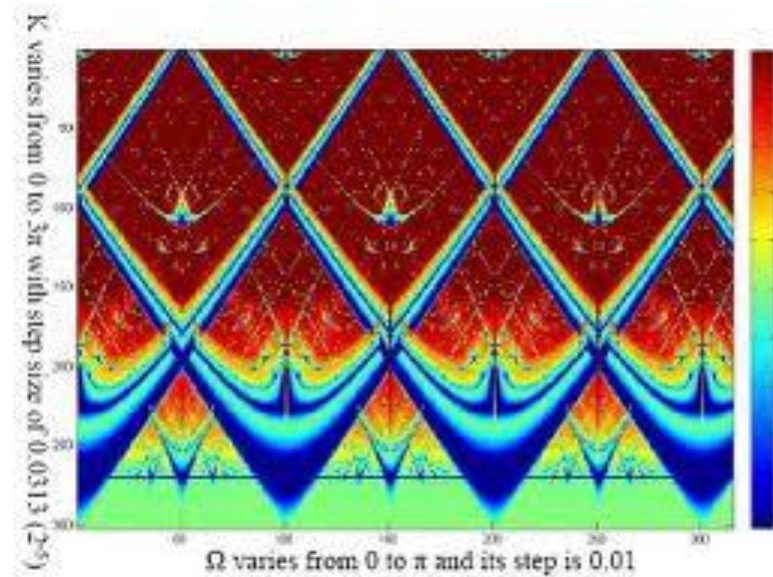
Two coupled oscillators: Arnold tongues

$$\omega/\Omega = P/Q$$





Examples of Arnold tongues !



Transition to chaos via mode-locking: Universal ! Therefore go to experiments!

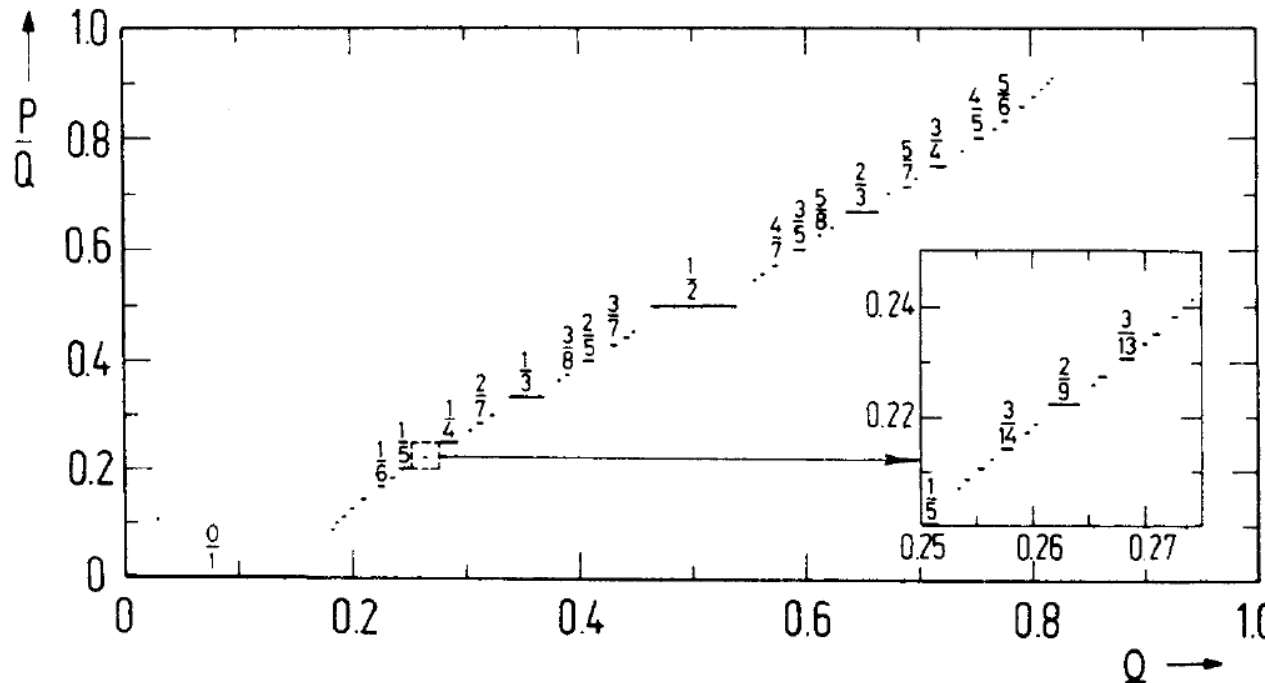


Figure 2. Devil's staircase: the mode-locking structure of the sine circle map at $K = 1$. The dressed winding numbers $P:Q$ are presented as a function of Ω . The self-similar (fractal) structure is exemplified by the inlay figure. From “Transition to Chaos by Interaction of Resonances in Dissipative Systems: I. Circle Maps,” by M. H. Jensen, P. Bak, and T. Bohr, 1984, *Physical Review A*, 30, p. 1962. Copyright 1984 by The American Physical Society. Adapted with permission.

Dimension= 0.8700....: Universal !



Ordering of Arnold tongues: Farey tree !

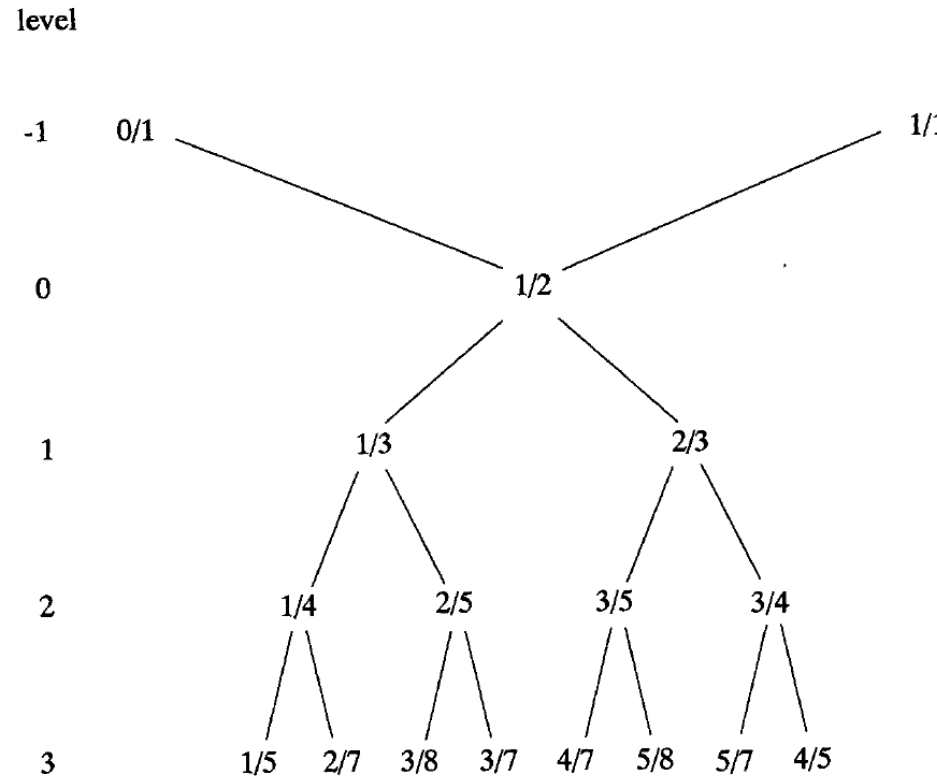


Figure 3. First five levels of the Farey tree.



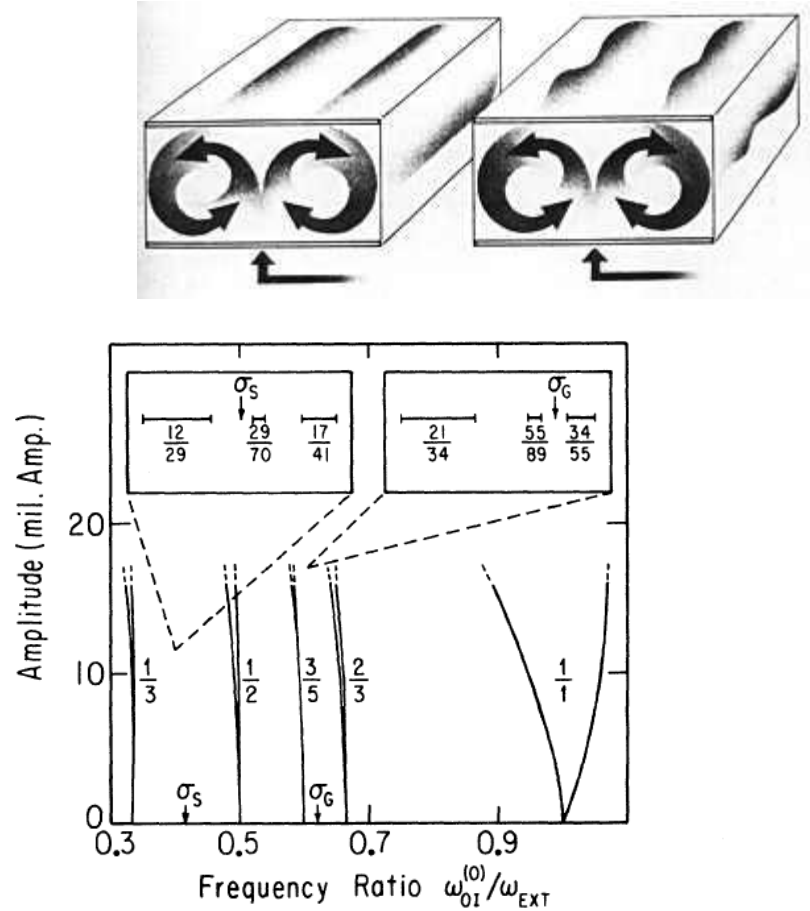


FIG. 1. Locked-mode regions (Arnold tongues) in a diagram of external pulse amplitude vs the ratio of the frequency of the oscillatory instability (at zero forcing) $\omega_{OI}^{(0)}$ to the frequency of the external pulses ω_{ext} . Only tongues of appreciable width are shown. The frequency ratio is given for these tongues. Insets: Locked states near σ_G and σ_S (Ref. 12) on the critical line. The origin of each inset shows the position of the critical line at the particular irrational frequency ratio and the precise frequency limits of each locked state are given in Table I.

(Jensen, Libchaber, Stavans,
Procaccia, Kadanoff, PRL)



Experimental attractor: Golden mean winding number!

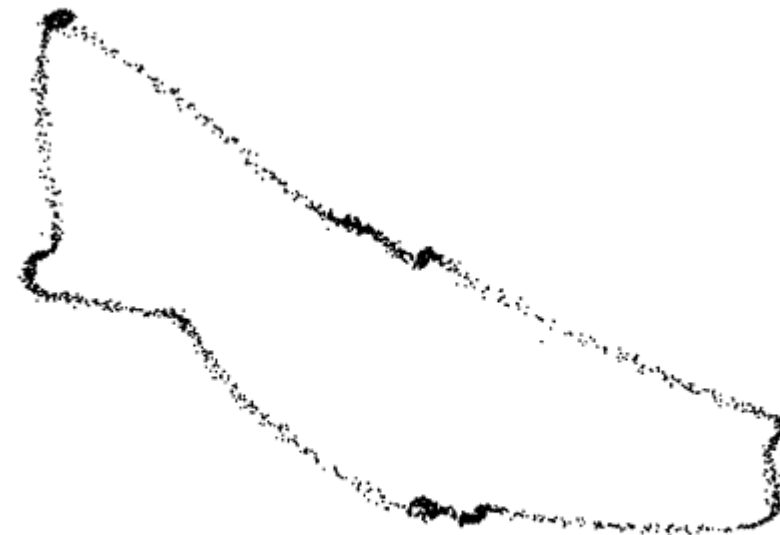


FIG. 1. The experimental attractor in two dimensions. 2500 points are plotted. Note the variation in the density of points on the attractor. Part of this variation is, however, due to the projection of the attractor onto the plane. The at-



Universal curve for modelocking: Experimental and theoretical results !

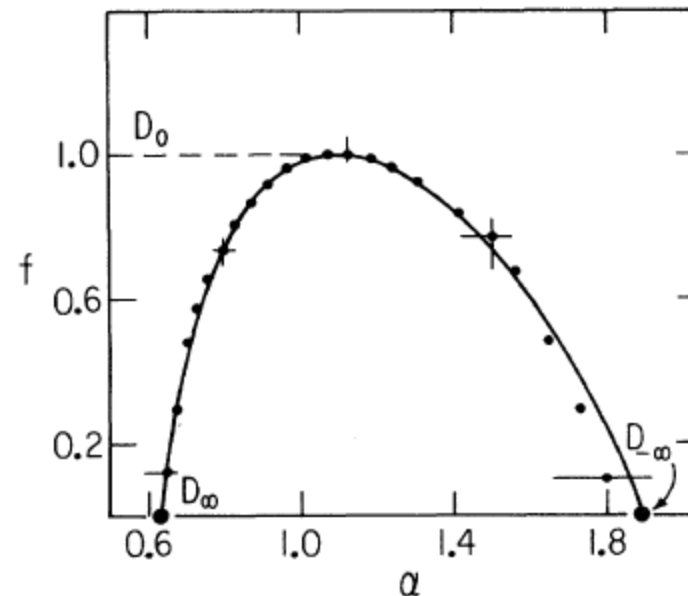
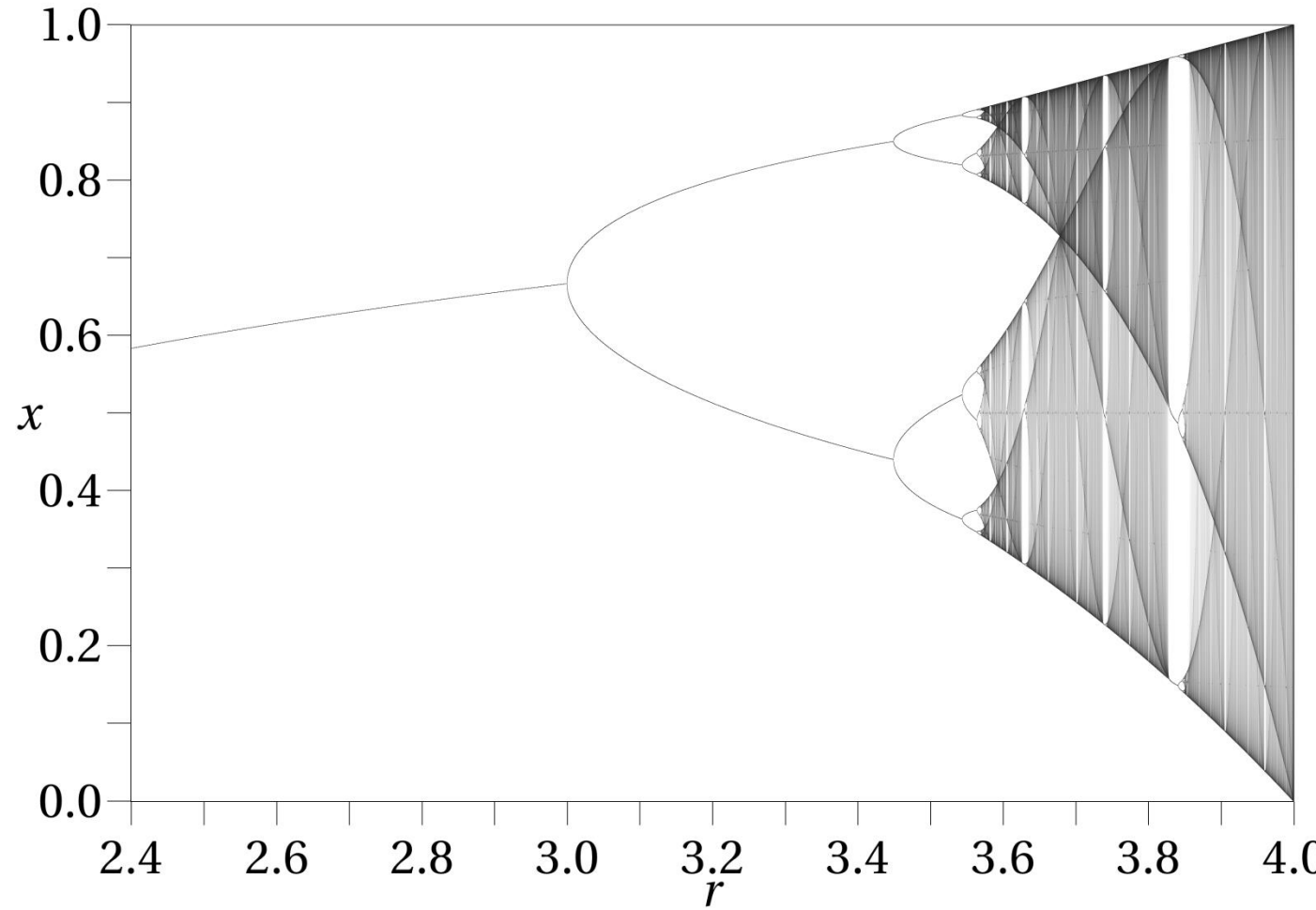


FIG. 2. The $f(\alpha)$ spectrum calculated for a critical circle map with golden-mean winding number is shown by the curve (Ref. 6). The curve ends in the points $(D_\infty, 0)$ and $(D_{-\infty}, 0)$, which are shown by the two large dots. The $f(\alpha)$ estimates for the experimental time series are marked by the smaller dots. The error bars are estimated by varying the range of l used to fit the data.

(Jensen, Libchaber, Stavans, Procaccia, Kadanoff, PRL)



Transition to chaos via period-doubling: Universal ! Therefore go to experiments !



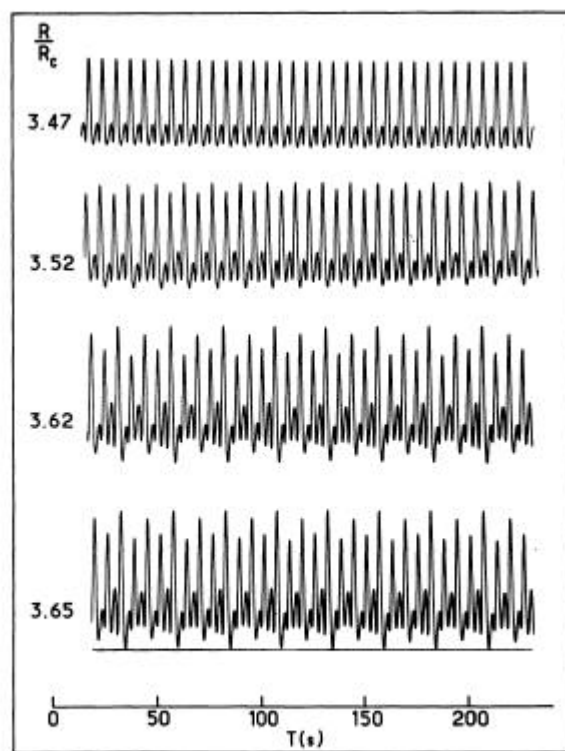
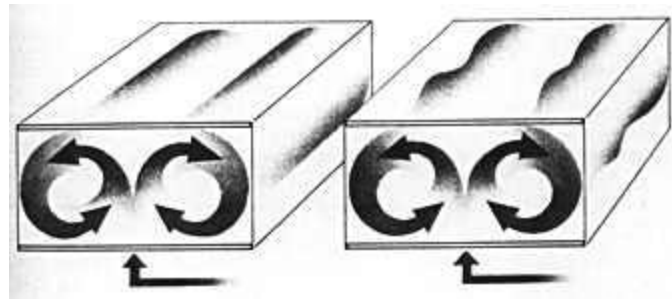


Fig. 2.— Direct time recordings of temperature for various stages of the period doubling cascade showing the onset of $f/4$ ($R/R_c = 3.52$), $f/8$ ($R/R_c = 3.62$), $f/16$ ($R/R_c = 3.65$).

L-214 JOURNAL DE PHYSIQUE — LETTRES

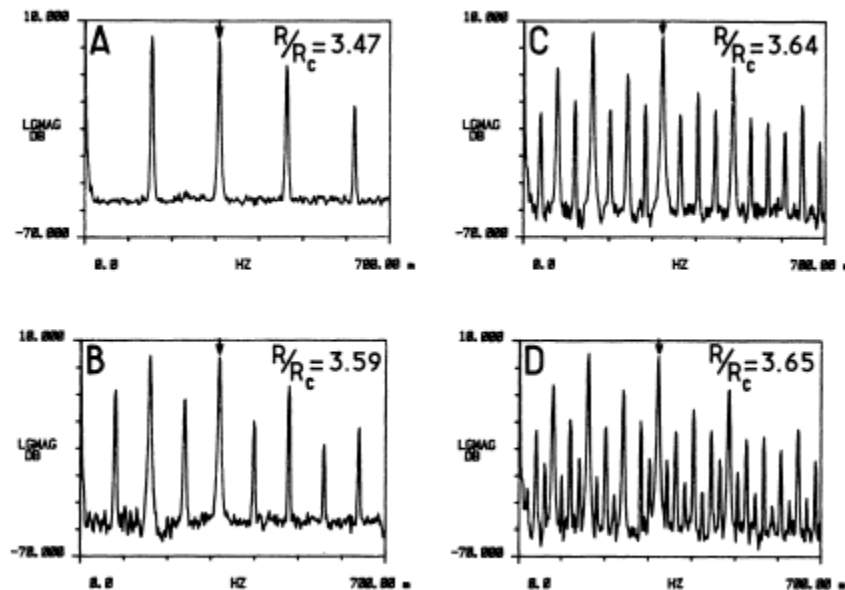


Fig. 3.— The Fourier spectrum. Arrows indicate the peak at the frequency f_1 .

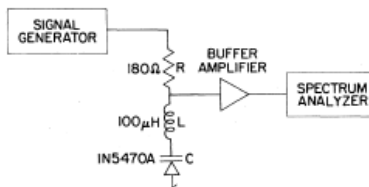


FIG. 1. Experimental apparatus for subharmonic generation.

Here V is the voltage across the diode and is positive for reverse bias. The measured values of capacity were in excellent agreement with this formula for the parameter values $C_0 = 81.8 \text{ pF}$, $\varphi = 0.6 \text{ V}$, and $\gamma = 0.44$. The circuit was driven sinusoidally from a signal generator with a $50\text{-}\Omega$ source impedance and the output was analyzed by a spectrum analyzer which measured the power contained in each spectral peak.

At very low drive voltages the circuit behaved as a linear RLC circuit with a resonance at $f_1 = 1.78 \text{ MHz}$. The nonlinear behavior was observed by driving the circuit at this frequency and gradually increasing the drive voltage. At low voltages the circuit displayed the frequency multiplication typical of all nonlinear circuits. The first subharmonic appeared at a drive voltage of 1.9 V . The saturated subharmonic peaks which appear at successive period doublings are shown in Figs. 2(a)-2(d). It is clear from the data that once a spectral peak has appeared and reached full magnitude it remains essentially unchanged through any further period doublings. In Fig. 2(d) the fundamental spectral peak is labeled 0, and the subharmonic peaks are labeled 1 through 4 according to their order of appearance after suc-

TABLE I. Measured value of the convergence rate δ .

Subharmonic	$\Delta V_{\text{threshold}}$ (V)	δ_n
$f_1/2$	3.2 ± 0.02	
$f_1/4$	0.72 ± 0.02	4.4 ± 0.1
$f_1/8$	0.16 ± 0.02	4.5 ± 0.6
$f_1/16$		

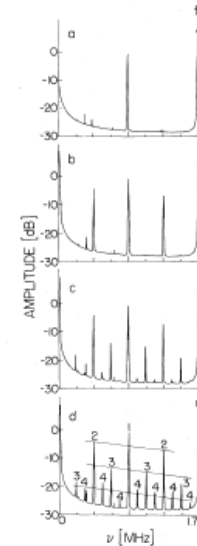


FIG. 2. (a)-(c) Subharmonic spectrum for successive period doublings; (d) final period doubling and comparison with theory.

cessive period doublings. The three lines in the figure are a straight line interpolating between the $n = 2$ peaks and two lines, respectively, 8.2 and 16.4 dB below it. The third and fourth generation spectral peaks are in remarkable agreement with the theoretical prediction. Noise in

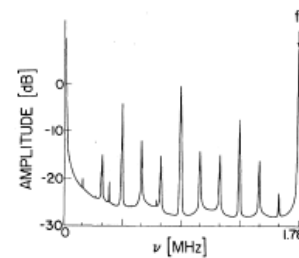
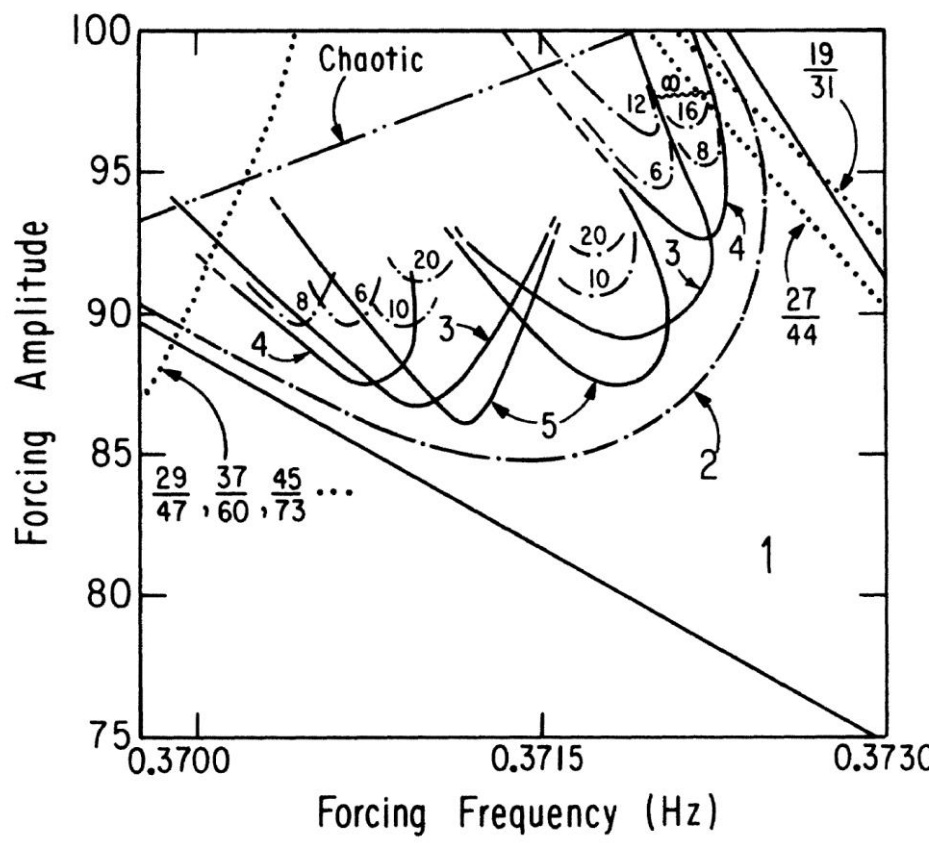


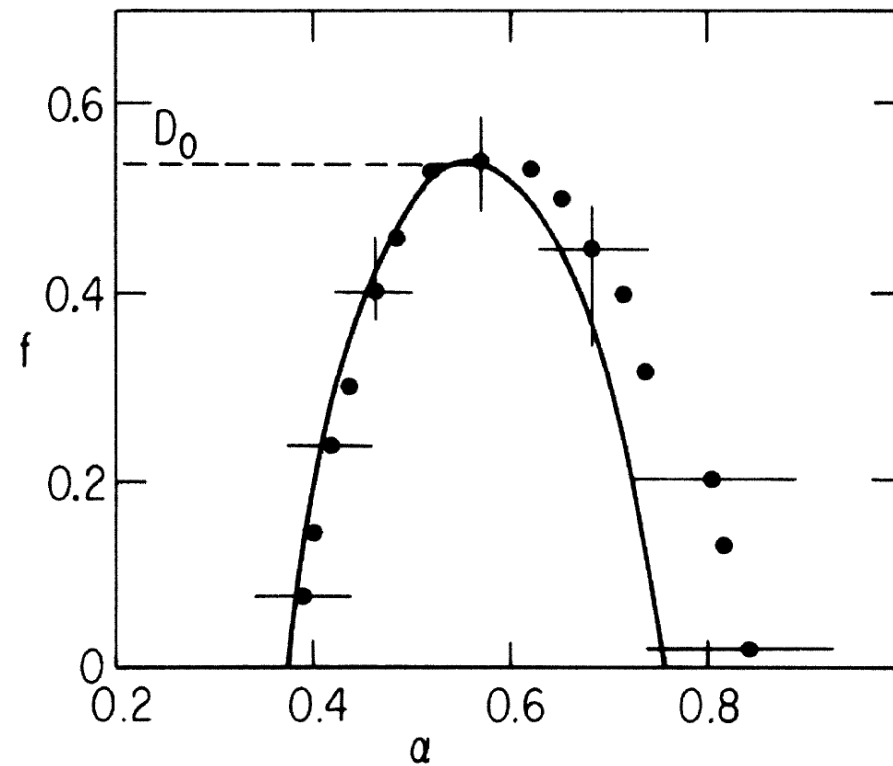
FIG. 3. Subharmonic spectrum prior to the onset of the chaotic spectrum.



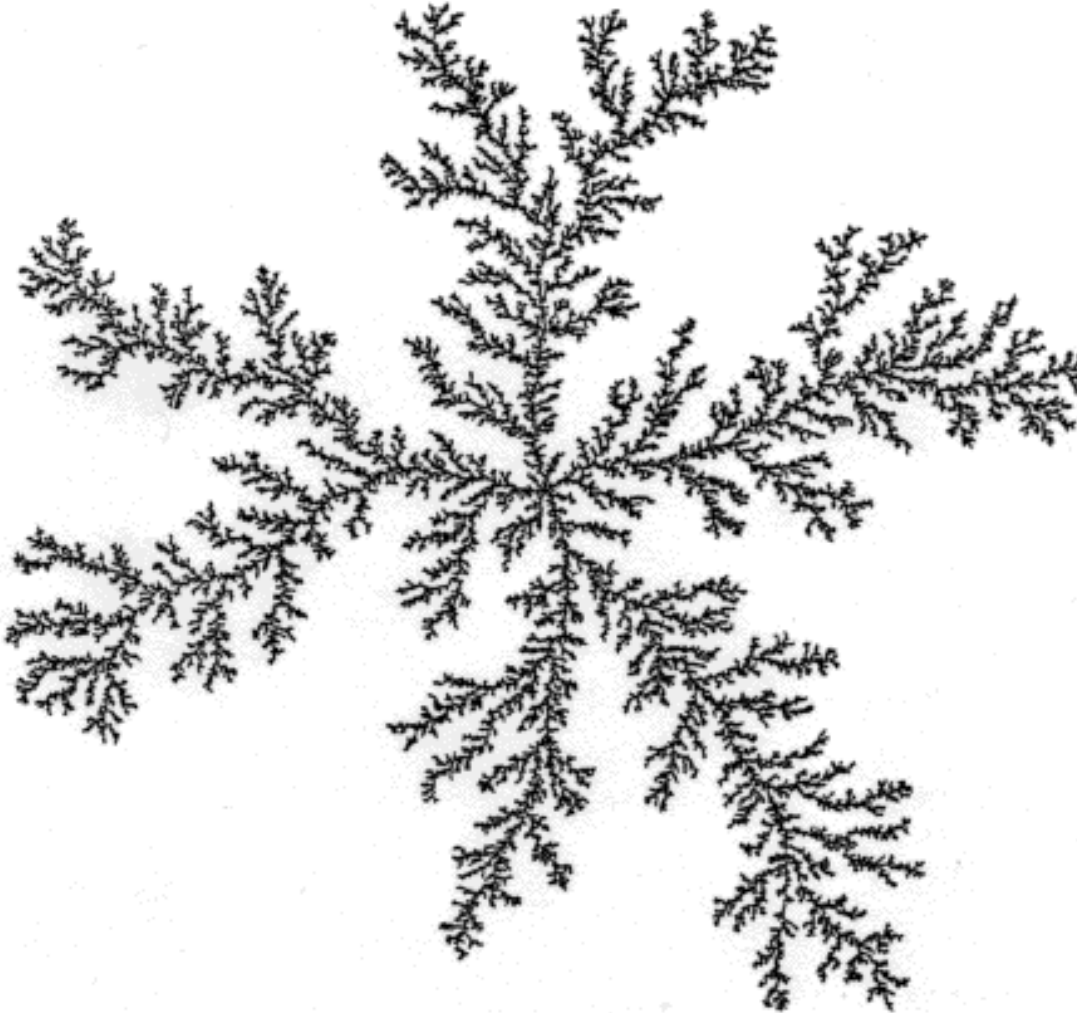
GLAZIER, JENSEN, LIBCHABER, AND STAVANS



Universal curve for period doubling: Experimental and theoretical results !



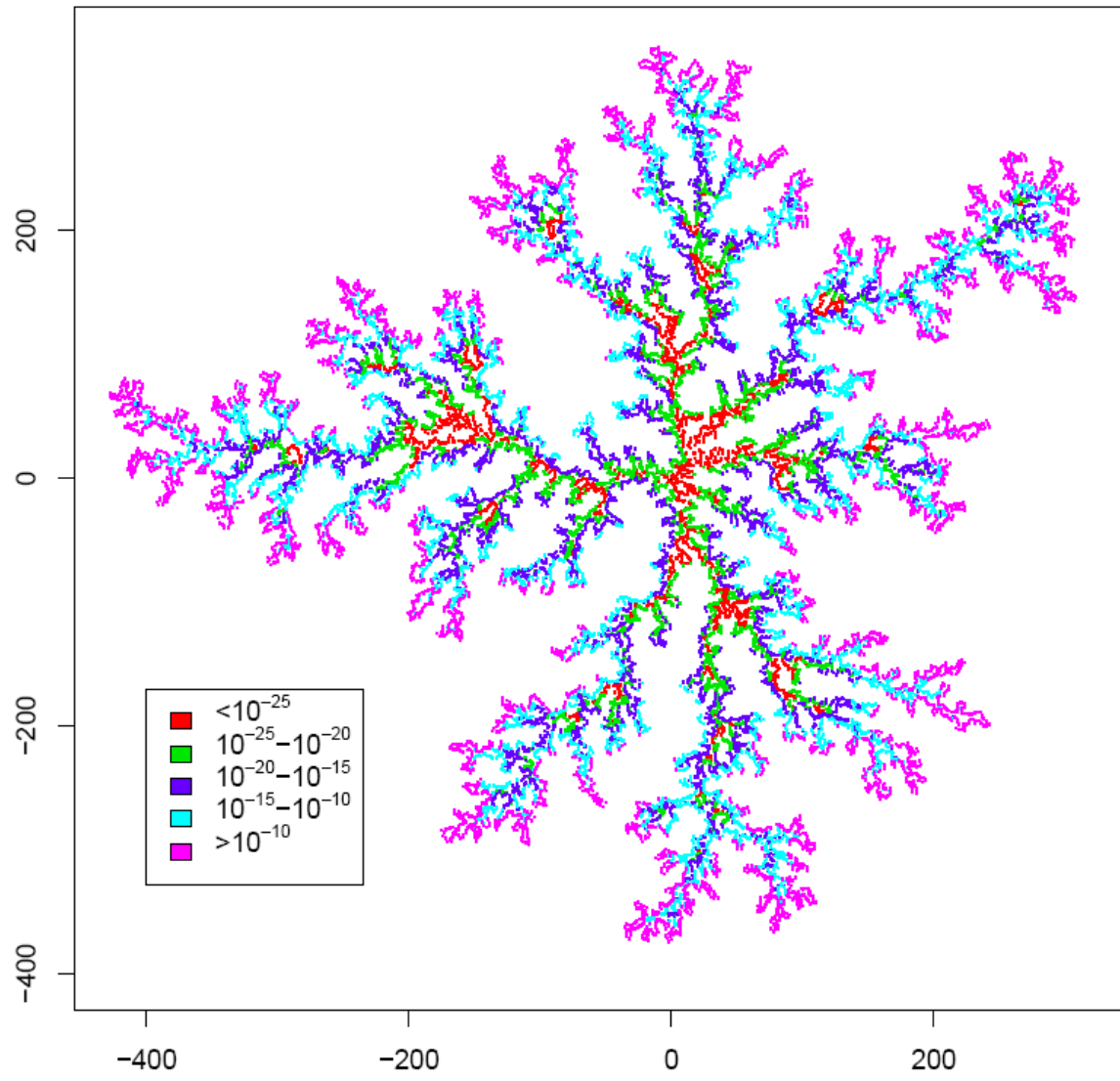
Diffusion Limited Aggregation



Self-similar on all scales !



Harmonic measure DLA (Mathiesen, Jensen)



DLA multifractal curves (Adams et al 2009)

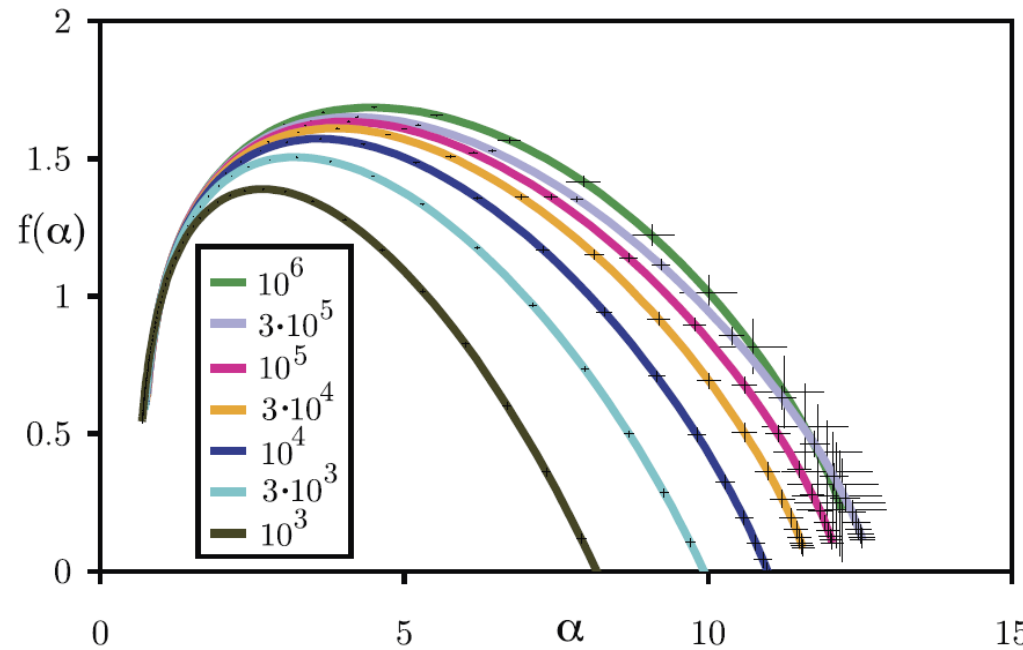
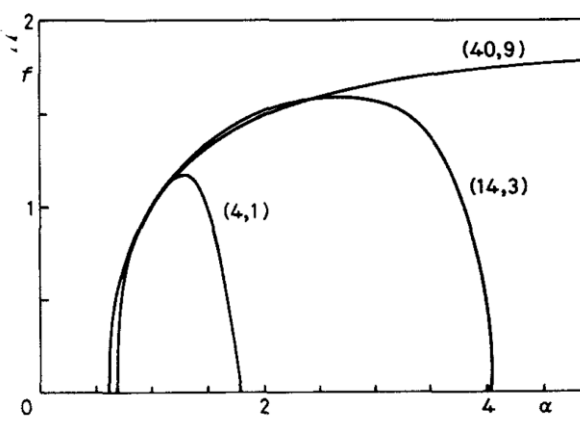
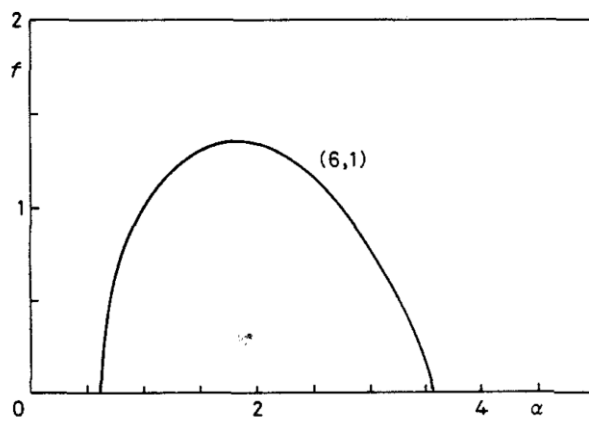
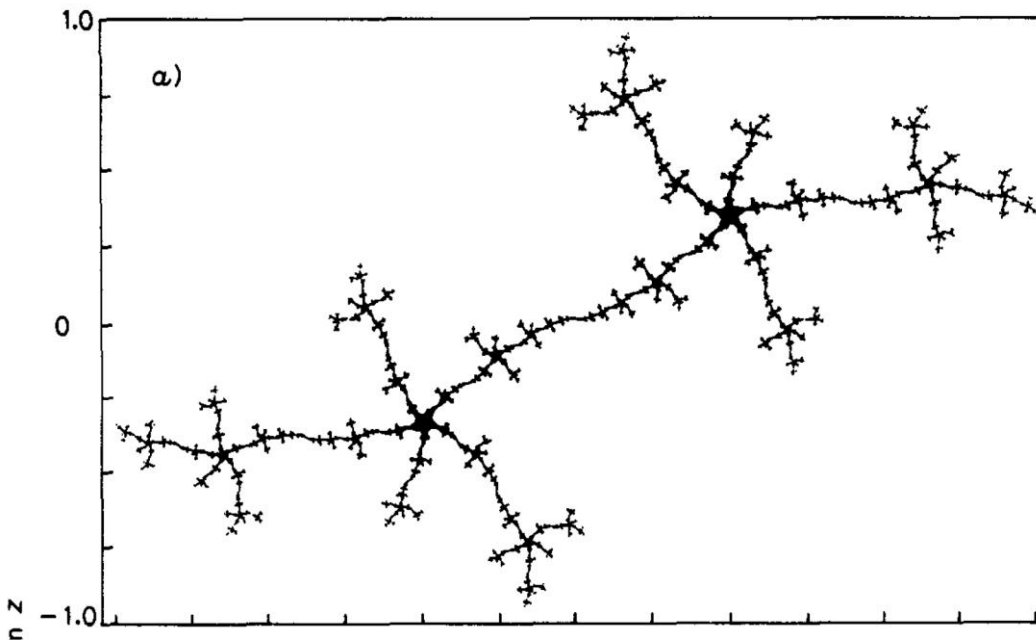


Fig. 3: (Color online) $f(\alpha)$ vs. α for seven different system sizes with error bars. Note that the spectra appear to be converging to some asymptotic spectrum.





This defines a “regular” Cantor set by the iterations of the fragmentation process, and we give again equal weights 2^{-n} to each of the 2^n intervals obtained at the n th step. However, it is possible consider the ensemble of realizations of these Cantor sets and look to the disorder average [over the distribution of the random variables l_1 and l_2 of the partition function (2)]

$$\langle \Gamma_n(q, \tau) \rangle = \int_0^1 dl_1 \frac{1}{1-l_1} \int_0^{1-l_1} dl_2 2^{-qn} (l_1^{-\tau} + l_2^{-\tau})^n \quad (5)$$

and determine $\tau_n(q)$ [and so $f_n(\alpha)$] by solving the equation $\langle \Gamma_n(q, \tau(q)) \rangle = 1$.

The explicit calculation of $\langle \Gamma_n(q, \tau) \rangle$ is rather interesting (see a similar result in [17]). The integral (5) does diverge for $\tau_n n \geq 1$, while for $\tau_n n \leq 1$ one obtains

$$\langle \Gamma_n \rangle = 2^{-nq} \sum_{k=0}^n \binom{n}{k} \frac{B(-\tau_n(n-k)+1, -\tau_n k+1)}{(1-\tau_n k)}, \quad (6)$$

where $B(x, y)$ is the Euler beta function. The conver-

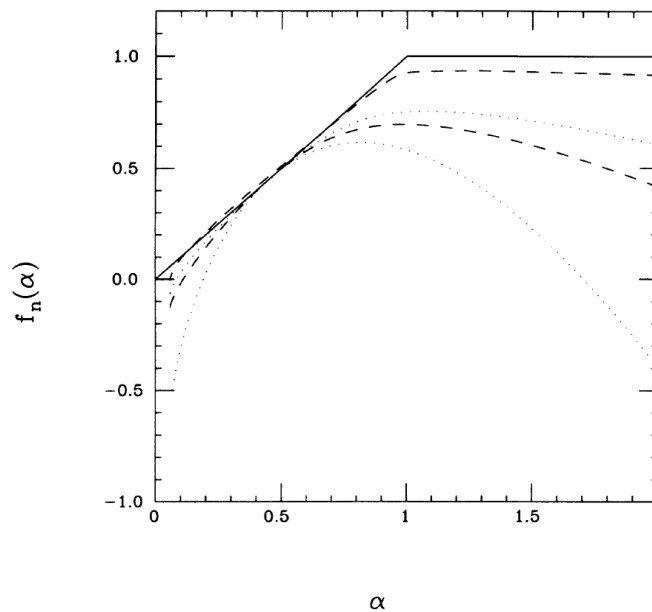


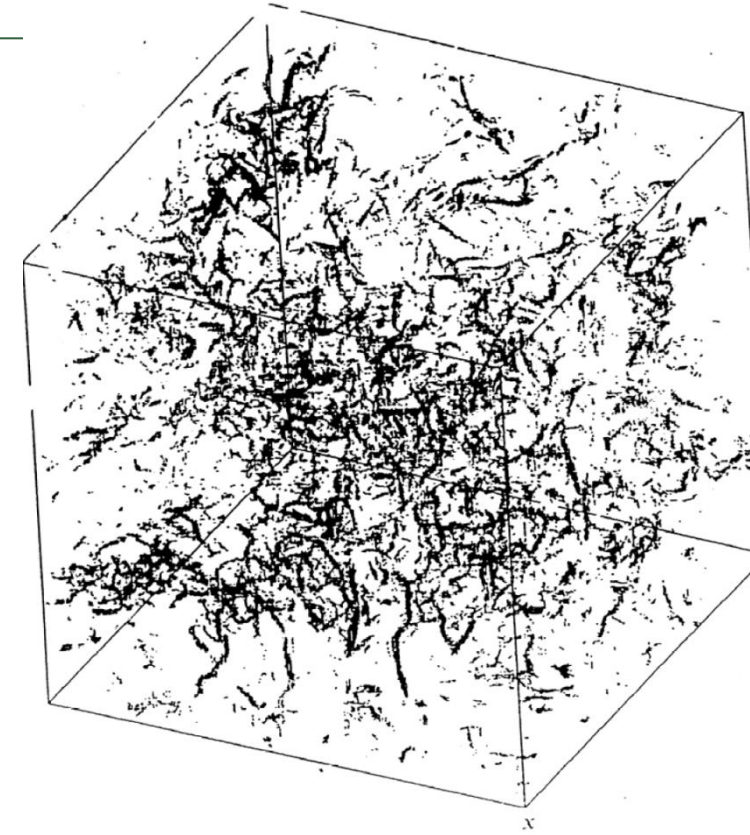
FIG. 1. $f(\alpha)$ versus α for $n=1$ (dotted line), $n=5$ (dashed line), $n=10$ (dotted line), and $n=100$ (dashed line), obtained by a Legendre transform of $\tau(q)$. The solid line is the convex envelope of the thermodynamic limit. The top of the spectrum is the fractal dimension $D_0(n)$.





Turbulence has Multifractal Nature

Faculty of Science



Navier-Stokes equations

$$\rho \left(\underbrace{\frac{\partial \mathbf{v}}{\partial t} + \mathbf{v} \cdot \nabla \mathbf{v}}_{\text{Unsteady acceleration}} + \underbrace{\mathbf{v} \cdot \nabla \mathbf{v}}_{\text{Convective acceleration}} \right) = \underbrace{-\nabla p}_{\text{Pressure gradient}} + \underbrace{\mu \nabla^2 \mathbf{v}}_{\text{Viscosity}} + \underbrace{\mathbf{f}}_{\text{Other forces}}$$

Inertia

Scientific paradigms

Single words, concepts: Nano, string theory, systems biology, climate change, chaos

Rapid growth → Slow decline

Scientific paradigms → Global awareness
(nanotechnology, climate change)

How does a person change 'his/her' opinion and concept?



Model ingredients

An 'infinity of concepts': A person **never** 'returns' to old concept

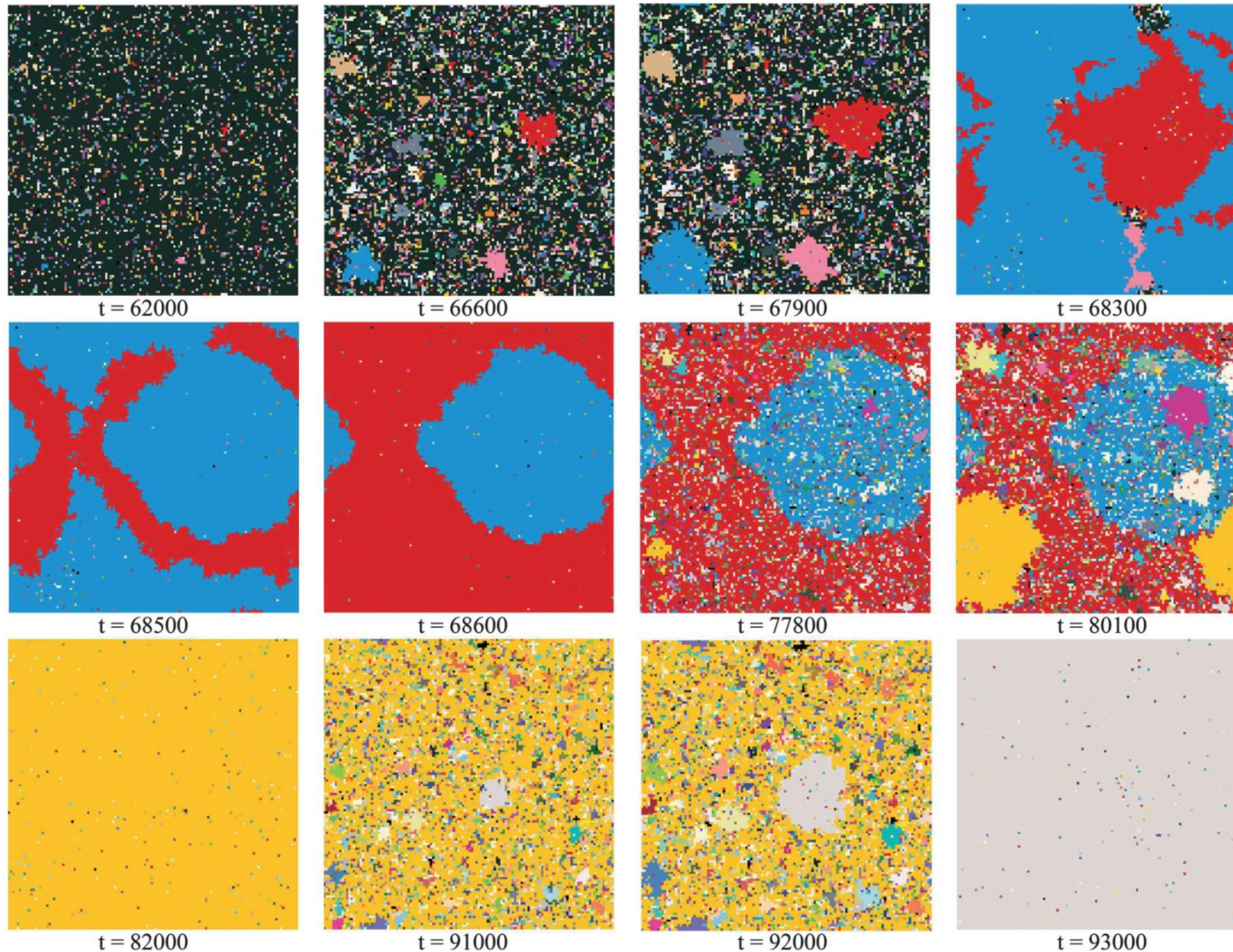
Cooperativity: A person change concept with a **weight** proportional to the '**size**' of the paradigm → A paradigm can 'flush' through the whole world !

Certain small probability **a** to change concept
(innovation rate)

Technically: $N=L \times L$ persons on a lattice, 4 neighbors, $a \sim 10^{-6}$, 'infinitely' many different concepts



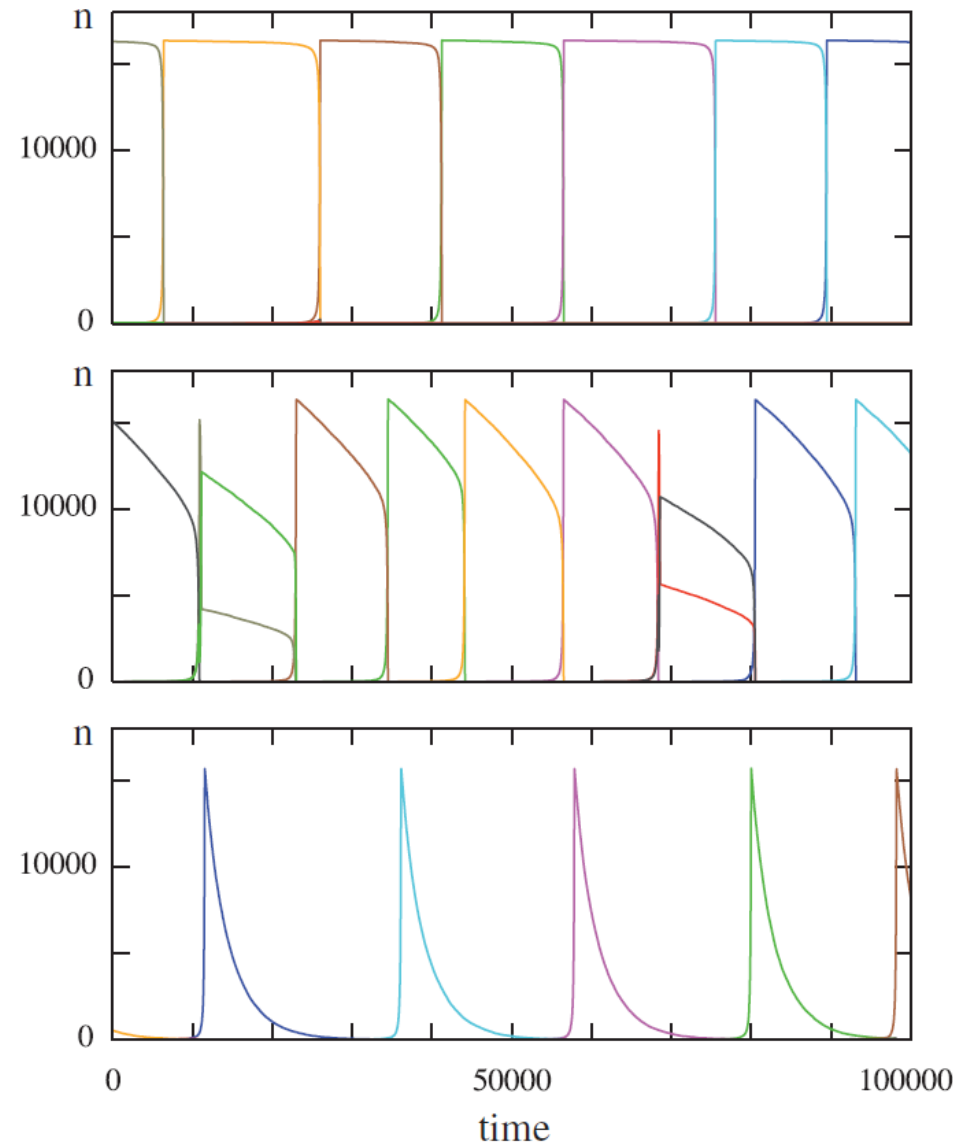
A paradigm/concept has one color



$N = 128 \times 128, \alpha \sim 25 \times 10^{-6}$, choose a neighbor, change according to weight



Time series of the dominant paradigm: Avalanches!



$$\alpha = 0.4 \times 10^{-6}$$

$$\alpha = 25 \times 10^{-6}$$

$$\alpha = 400 \times 10^{-6}$$

Nearly constant temporal 'epoch' independent of α



Number of visited sites

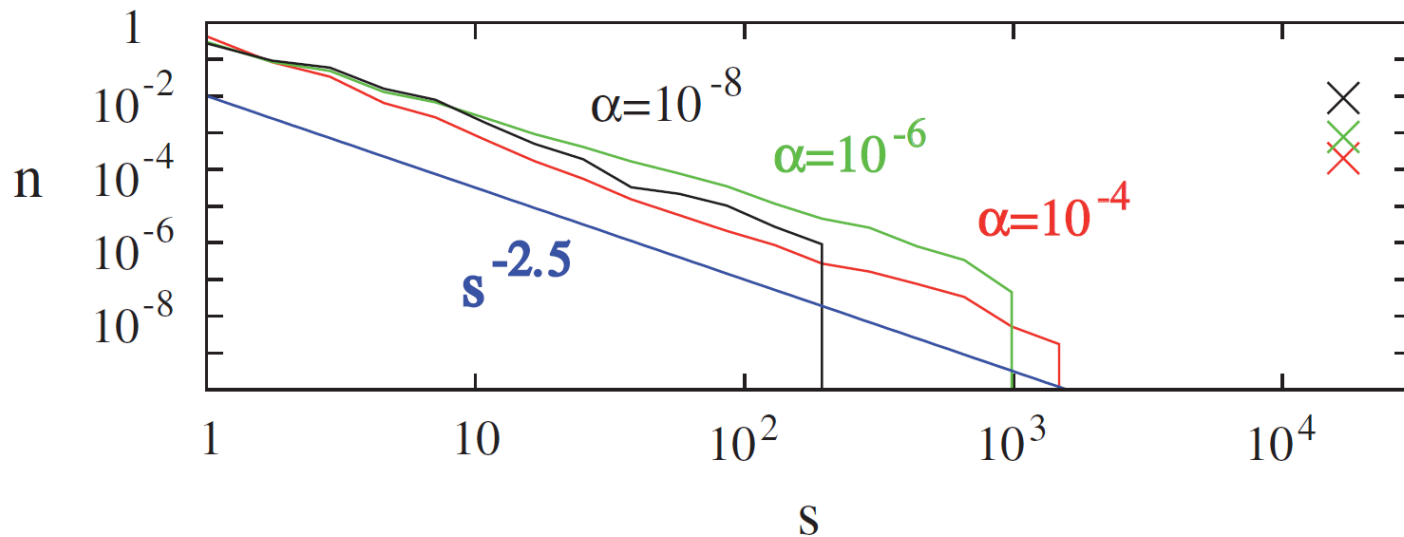


FIG. 4 (color). Distribution of the number of sites s that a particular idea visits during its life span for different values of α . Scaling $\sim 1/s^{2.5}$ for comparison (blue line). Note the gap between the main part of the distribution and the bins counting the ideas with system-wide sweeps (crosses). System size is $N = 128 \times 128$.

